

HumanoidBench: Simulated Humanoid Benchmark for Whole-Body Locomotion and Manipulation

Carmelo Sferrazza¹ Dun-Ming Huang¹ Xingyu Lin¹ Youngwoon Lee^{1,2} Pieter Abbeel¹
UC Berkeley¹ Yonsei University²

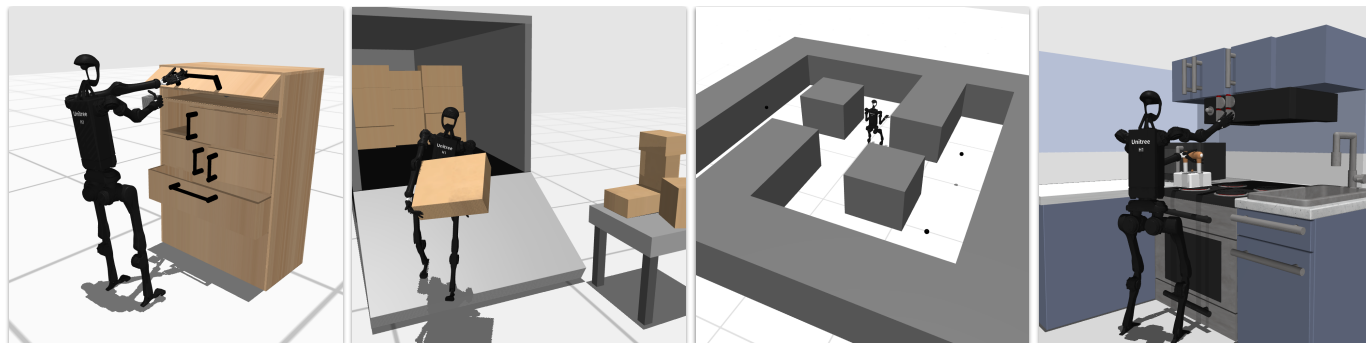


Fig. 1: Humanoid robots equipped with dexterous hands hold immense promise for integration into real-world human environments. Nonetheless, harnessing the full potential of humanoid robots presents numerous challenges, such as the intricate control of robots with complex dynamics, sophisticated coordination among various body parts, and addressing long-horizon complex tasks envisioned for these robots. We present **HumanoidBench**, a simulated humanoid robot benchmark consisting of 15 whole-body manipulation and 12 locomotion tasks, such as shelf rearrangement, package unloading, and maze navigation.

Abstract—Humanoid robots hold great promise in assisting humans in diverse environments and tasks, due to their flexibility and adaptability leveraging human-like morphology. However, research in humanoid robots is often bottlenecked by the costly and fragile hardware setups. To accelerate algorithmic research in humanoid robots, we present a high-dimensional, simulated robot learning benchmark, **HumanoidBench**, featuring a humanoid robot equipped with dexterous hands and a variety of challenging whole-body manipulation and locomotion tasks. Our findings reveal that state-of-the-art reinforcement learning algorithms struggle with most tasks, whereas a hierarchical learning baseline achieves superior performance when supported by robust low-level policies, such as walking or reaching. With **HumanoidBench**, we provide the robotics community with a platform to identify the challenges arising when solving diverse tasks with humanoid robots, facilitating prompt verification of algorithms and ideas. The open-source code is available at https://sferrazza.cc/humanoidbench_site.

I. INTRODUCTION

Humanoid robots have long held promise to be seamlessly deployed in our daily lives. Despite the rapid progress in humanoid robots’ hardware (e.g., Boston Dynamics Atlas, Tesla Optimus, Unitree H1), their controllers are fully or partially hand-designed for specific tasks, which requires significant engineering efforts for each new task and environment, and often demonstrates only limited whole-body control capabilities.

In recent years, robot learning has shown steady progress in both robotic manipulation [10, 61, 12] and locomotion [23, 63]. However, scaling learning algorithms to humanoid robots is

still challenging and has been delayed mainly due to such robots’ costly and unsafe real-world experimental setups.

To accelerate the progress of research for humanoid robots, we present the first-of-its-kind humanoid robot benchmark, **HumanoidBench**, with a diverse set of locomotion and manipulation tasks. Our simulated humanoid benchmark demonstrates a variety of challenges in addressing learning for autonomous humanoid robots, such as the intricate control of robots with complex dynamics, sophisticated coordination among various body parts, and addressing long-horizon complex tasks, while providing an accessible, fast, safe, and inexpensive testbed to robot learning researchers.

HumanoidBench contributes (1) a simulation environment comprising a humanoid robot with two dexterous hands, as illustrated in Figure 1; (2) a variety of tasks, spanning locomotion, manipulation, and whole-body control, incorporating humans’ everyday tasks; (3) a standardized benchmark to evaluate the progress of the community on high-dimensional humanoid robot learning and control; and finally, (4) benchmarking results of the state-of-the-art reinforcement learning (RL) algorithms and a hierarchical RL approach.

The simulation environment of **HumanoidBench** uses the MuJoCo [52] physics engine. For the simulated humanoid robot, we mainly opt for a Unitree H1 humanoid robot¹, which is relatively affordable and offers accurate simulation models [58],

¹<https://www.unitree.com/h1>

Benchmark	Dexterous hands	Action dim.	DoF	Task horizon	# Tasks	Skills ¹
MyoHand [7]	✓	39	23D	50-2000	9	PnP, R, Po, IR, H, Ro
Adroit [42]	✓	24	24D	200	4	PnP, P, R, Po, IR, H, L, Ro
MyoLeg [7]	✗	80	20D	1000	1	Lo, St
LocoMujoco [3] (Unitree-H1)	✗	19	6D	100-500	27	L, Lo, St, BM
DMControl [50]	✗	24 or 56	22D	1000	6	Lo, St
FurnitureSim [19]	✗	8	6D	2300	8	PnP, P, I, IR, H, L, Ro
robosuite [62]	✗	6-24	6-7D	500	9	PnP, P, I, R, IR, H, L, Ro
ribench [21]	✗	6-7	6-7D	100-1000	106	PnP, P, I, R, Po, IR, H, L, Ro
metaworld [56]	✗	6	7D	500	50	PnP, P, I, R, Po, IR, H, L, Ro
HumanoidBench (Ours)	✓	61	101D	500 – 1000	16	PnP, P, I, R, Po, IR, H, L, Ro, Lo, BM, St

¹PnP: Pick-and-place / P: Push / I: Insert / R: Reach / Po: Pose / IR: In-hand re-orientation / H: Hold / L: Lift / Ro: Rotate / Lo: Locomotion / BM: Whole-body (humanoid) Manipulation / St: Stabilization

TABLE I: **Comparison of simulated robotic manipulation benchmarks.** Our humanoid robot benchmark tests a variety of complex, long-horizon task with a large action space.

with two dexterous Shadow Hands² attached to its arms. Our environment can easily incorporate any humanoid robots and end effectors; thus, we provide other models, including Agility Robotics Digit³ and the Robotiq 2F-85 gripper.

The HumanoidBench task suite includes 15 distinct whole-body manipulation tasks involving a variety of interactions, e.g., unloading packages from a truck, wiping windows using a tool, catching and shooting a basketball. In addition, we provide 12 locomotion tasks (not requiring hands’ dexterity), which can serve as primitive skills for whole-body manipulation tasks and provide a set of easier tasks to verify algorithms. The benchmarking results on this task suite show how the state-of-the-art RL algorithms struggle with controlling the complex humanoid robot dynamics and solving the most challenging tasks, illustrating ample opportunities for future research.

II. RELATED WORK

Deep reinforcement learning (RL) has made rapid progress with the advent of standardized, simulated benchmarks, such as Atari [4] and continuous control [6, 50] benchmarks. In robotic manipulation, most existing simulated environments are limited to quasi-static, short-horizon skills, having focused on tasks like picking and placing [6, 21, 62, 56, 32], in-hand manipulation [42, 38, 7], and screwing [37].

Complex manipulation tasks, such as block stacking [11], kitchen tasks [14], and table-top manipulation [22, 34, 29], have been introduced but are still limited to a combination of pushing, picking, and placing. On the other hand, the IKEA furniture assembly environment [27], BEHAVIOR [48, 28], and Habitat [49] present diverse long-horizon (mobile) manipulation tasks, with their main focus being on high-level planning by abstracting complex low-level control problems, while FurnitureBench [19] introduces a simulated benchmark for complex long-horizon furniture assembly tasks with sophisticated low-level control. However, most of these benchmarks use a single-arm manipulation setup with either a parallel gripper or a dexterous hand [8, 42], limiting the types of object interactions

and not addressing the challenges of coordinating multiple parts of a body [26], e.g., multiple fingers, arms, and legs.

Robosuite [62] includes a handful of bimanual manipulation tasks, while more recently [9] and [59] have introduced additional benchmarks that require coordinating two floating robot hands, i.e., not attached to any arm base. While bimanual manipulation is one of the key objectives of humanoid robots, most benchmarks in humanoid research have so far focused on the locomotion challenges of such platforms [7, 24, 39, 3]. In this regard, such simulations have accelerated research on control algorithms [5, 40, 41, 35], ultimately leading to achieve robust humanoid locomotion in the real world [1, 43].

Recent works have extended humanoid simulations to different domains involving a certain degree of manipulation, i.e., tennis [60], soccer [16], ball manipulation [53] and catching [33], and box moving [55]. However, all these works focus on demonstrating their approaches on specific humanoid tasks and lack a diversity of tasks. In addition, most of the previous work focuses on simplistic humanoid models [33, 53], leading to inaccurate physics and collision handling. This motivates us to implement a *comprehensive* simulated humanoid benchmark based on real-world hardware and consisting of a diverse set of whole-body control tasks with careful design choices for diversity and usability.

III. SIMULATED HUMANOID ROBOT ENVIRONMENT

In this section, we describe our simulated environment and discuss relevant design choices for the simulated humanoid robot. As illustrated in Figure 2, we use the Unitree H1 humanoid robot¹ with two dexterous Shadow Hands² as the primary robotic agent of our benchmark. We simulate this humanoid robot using MuJoCo [52] adapting the Unitree H1 model provided by Unitree⁴ and the dexterous Shadow Hand models available through MuJoCo Menagerie [58].

Humanoid Body. We implement Unitree H1¹ and Agility Robotics Digit³, which are well-known humanoid robots with their model files freely available [58]. Unitree H1 is primarily used in our benchmark as we observed faster learning, which we ascribe to a simpler mechanical design compared to Agility

²<https://www.shadowrobot.com/dexterous-hand-series/>

³<https://agilityrobotics.com/robots>

⁴https://github.com/unitreerobotics/unitree_ros

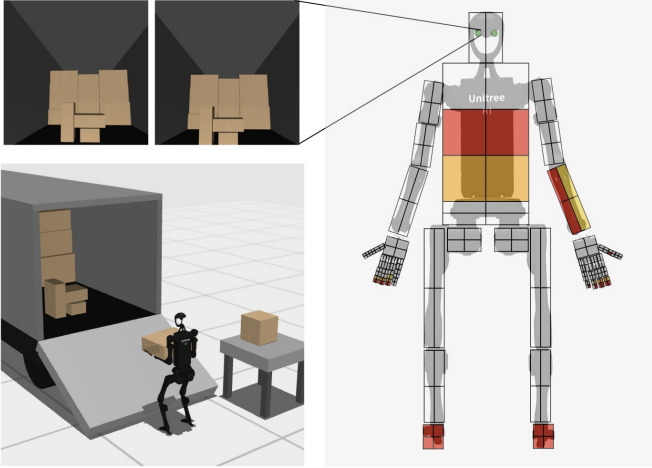


Fig. 2: Example egocentric visual (top-left) and whole-body tactile (right) observations when the humanoid interacts with a package in the `truck` environment. In the right figure, the two cameras on the robot head are highlighted in green, while continuous tactile pressure readings are indicated in shades of red and yellow. Note that here, for ease of visualization, we are not showing shear forces and tactile readings on the back of the robot, which are also implemented in our environment.

Robotics Digit, which features passive joints actuated through a four-bar linkage.

Dexterous Hands. We use two dexterous Shadow Hands², which also have model files freely available [58], and have shown impressive manipulation capabilities both in simulation [59] and the real world [2]. To make the simulated robot have more human-like morphology, we remove the cumbersome forearms of the dexterous Shadow Hands in HumanoidBench. While this is not currently a realistic model, we anticipate the trend in the industry towards developing slimmer, human-like hands (e.g. Tesla Optimus, Figure 01) so that our design choice aligns better with next-generation humanoid robots. In addition, we also provide models for the Robotiq 2F-85 parallel-jaw gripper and the hands available in the Unitree collection⁴.

Observations. Our simulated environment supports the following observations:

- Proprioceptive robot state (i.e. joint angles and velocities) and task-relevant environment observations (i.e. object poses and velocities).
- Egocentric visual observations from two cameras placed on the robot head (see Figure 2).
- Whole-body tactile sensing using the MuJoCo tactile grid sensor (see Figure 2). We design tactile sensing at the hands with high resolution and in other body parts with low resolution, similar to humans, with a total of 448 taxels spread over the entire body, each providing three-dimensional contact force readings. Similar distributed force readings have been captured on real-world systems both on humanoid bodies [36] and end-effectors [46]. The implementation of such spatially distributed contact sens-

ing required non-trivial mesh adaptations and refinements, which we detail in the appendix.

Although other sensory inputs are available from the environment, to investigate challenges in whole-body control of humanoid robots, we first focus on the state-based environment setup, where proprioceptive robot states and object states are used for the agent’s input in HumanoidBench. We leave extending our environment to benchmarking multimodal perception capabilities [57, 47] of humanoid robots as future work. Note that in our state-based environment, we essentially maintain the robot observations the same across tasks to minimize domain knowledge, in contrast to tailoring it to the specific tasks [51].

Actions. In our HumanoidBench experiments, the humanoid robot is controlled via position control (i.e., specifying the target joint positions). Torque-based control is also supported but we found that position control is generally more stable and allows for lower control frequency than torque control. For both position and torque control, the action space is 61-dimensional including the two hands, and controlled at 50 Hz.

IV. HUMANOIDBENCH

Humanoid robots promise to solve human-like tasks in human-tailored environments, possibly using human tools. However, their form factor and hardware challenges make real-world research challenging, making simulation a crucial tool to advance algorithmic research in the field.

To this end, we present HumanoidBench, a humanoid benchmark for robot learning and control, which features a high-dimensional action space (up to 61 different actuator) and enables research in complex whole-body coordination.

We benchmark 27 tasks, consisting of 12 locomotion tasks and 15 distinct manipulation tasks, as illustrated in Figure 4 and Figure 3. A set of locomotion tasks aim to provide interesting but simpler humanoid control scenarios, bypassing intricate dexterous hand control. On the other hand, whole-body manipulation tasks render a comprehensive evaluation of the state-of-the-art algorithms on challenging tasks with unique challenges that require coordination across the entire robot body, ranging from toy examples (e.g. pushing a box on a table) to practical applications (e.g. truck unloading, shelf rearrangement).

Below we briefly describe the tasks that are part of the benchmark. Further details about each of the tasks, including task initialization and reward functions, are provided in the appendix.

A. Locomotion Tasks

- `walk`: Keep forward velocity close to 1m/s without falling to the ground.
- `stand`: Maintain a standing pose throughout the provided amount of time.
- `run`: Run forward (in the global x -direction) at a speed of 5m/s.
- `reach`: Reach a randomly initialized 3D point with the left hand.

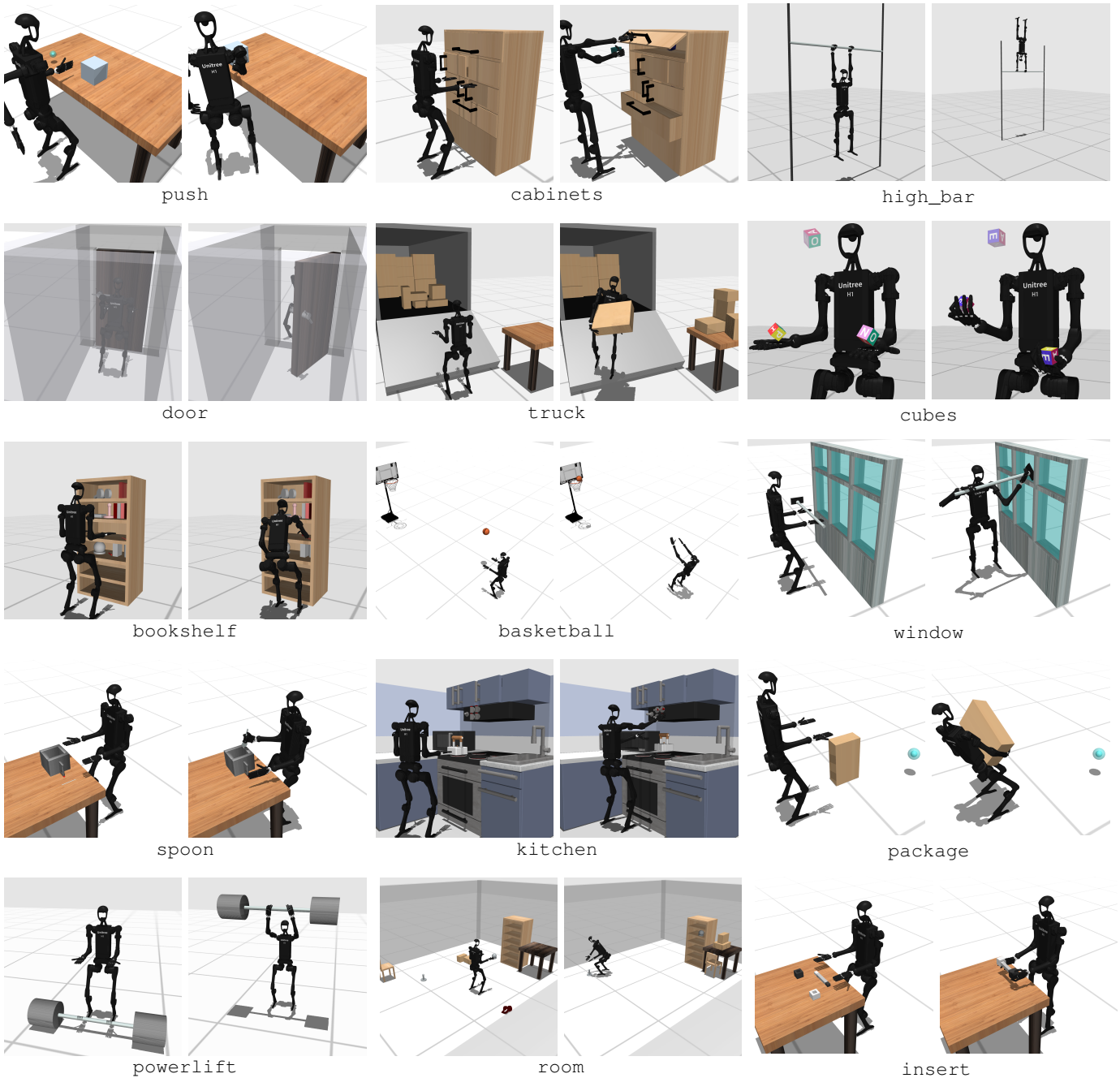


Fig. 3: **HumanoidBench manipulation task suite.** We devise 15 benchmarking whole-body manipulation tasks that cover a wide variety of interactions and difficulties. This figure illustrates an initial state (left) and target state (right) for each task.

- hurdle: Keep forward velocity close to 5 m/s while successfully overcoming hurdles.
- crawl: Keep forward velocity close to 1 m/s while passing inside a tunnel.
- maze: Reach the goal position in a maze by taking multiple turns at the intersections.
- sit: Sit onto a chair situated closely behind the robot.
- balance: Stay balanced on the unstable board.
- stair: Traverse an iterating sequence of upward and downward stairs at 1 m/s.

- slide: Walk over an iterating sequence of upward and downward slides at 1 m/s.
- pole: Travel in forward direction over a dense forest of high thin poles, without colliding with them.

B. Whole-Body Manipulation Tasks

- push: Move a box to a randomly initialized 3D point on a table.
- cabinet: Open four different types of cabinet doors (e.g. hinge doors, sliding door, drawer).

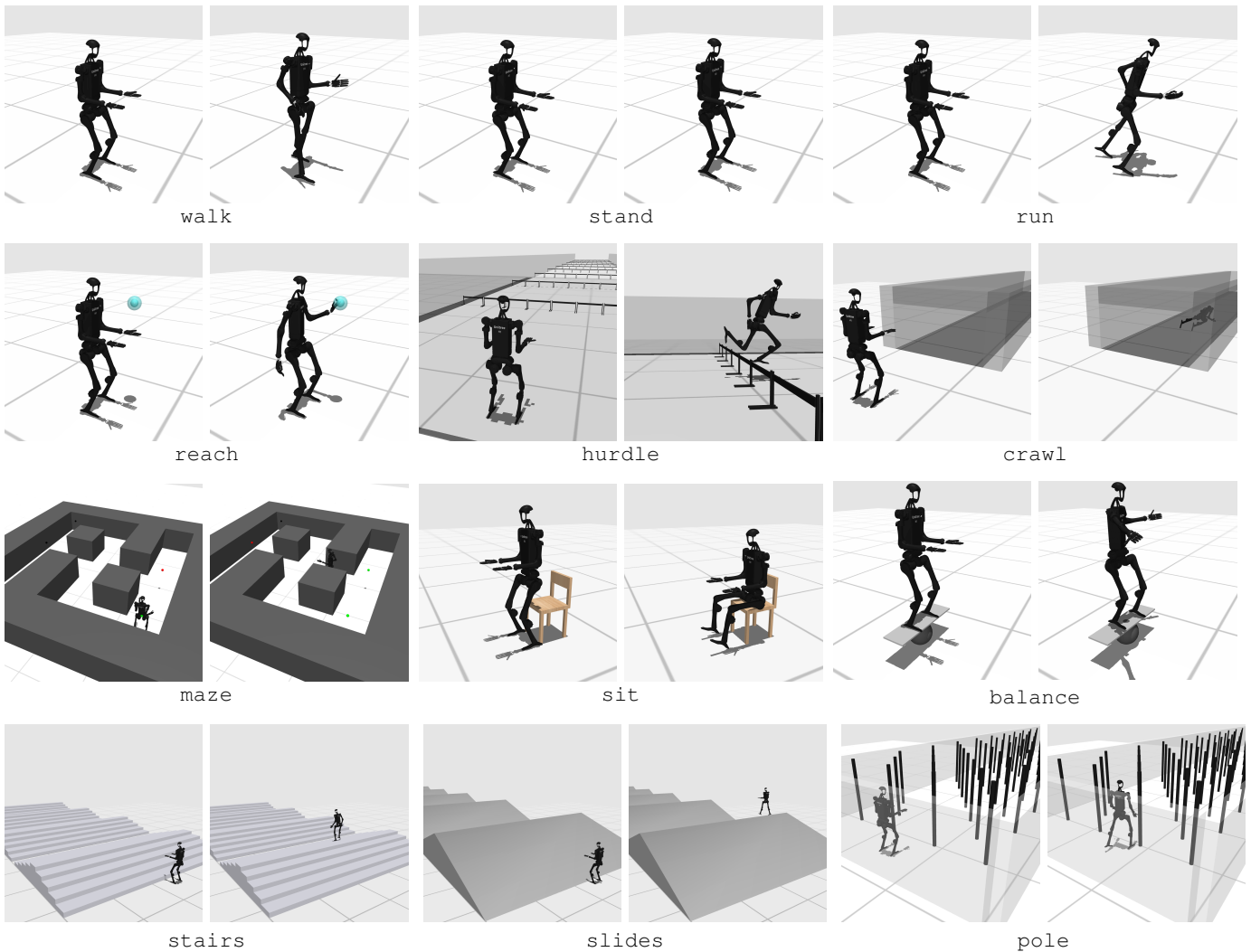


Fig. 4: **HumanoidBench locomotion task suite.** We devise 12 benchmarking locomotion tasks that cover a wide variety of interactions and difficulties. This figure illustrates an initial state (left) and target state (right) for each task, except for walk.

- **highbar**: Athletically swing while staying attached to a horizontal high bar until reaching a vertical upside-down position.
- **door**: Pull a door and traverse it while keeping the door open.
- **truck**: Unload packages from a truck by moving them onto a platform.
- **cube**: Manipulate two cubes in-hand until they both reach a randomly initialized target orientation.
- **bookshelf**: Pick and place several items across shelves in a given order.
- **basketball**: Catch a ball coming from random directions and throw it into the basket.
- **window**: Grab a window wiping tool and keep its tip parallel to a window by following a prescribed vertical velocity.
- **spoon**: Grab a spoon and use it to follow a circular pattern inside a pot.
- **kitchen** [14]: Execute a sequence of actions in a kitchen environment, namely, open a microwave door, move a kettle, and turning burner and light switches.
- **package**: Move a box to a randomly initialized target position.
- **powerlift**: Lifting a barbell shaped object of a designated mass.
- **room**: Organize a 5m by 5m space populated with randomly scattered object to minimize the variance of scattered objects' locations in x , y -axis directions.
- **insert**: Insert the ends of a rectangular peg into two tight target blocks.

V. BENCHMARKING RESULTS

To identify the challenges in learning with humanoid robots, we benchmark reinforcement learning (RL) algorithms on HumanoidBench, which promises for robots to learn from their own experience. Remarkably, this class of algorithms requires limited domain expertise and does not necessarily rely

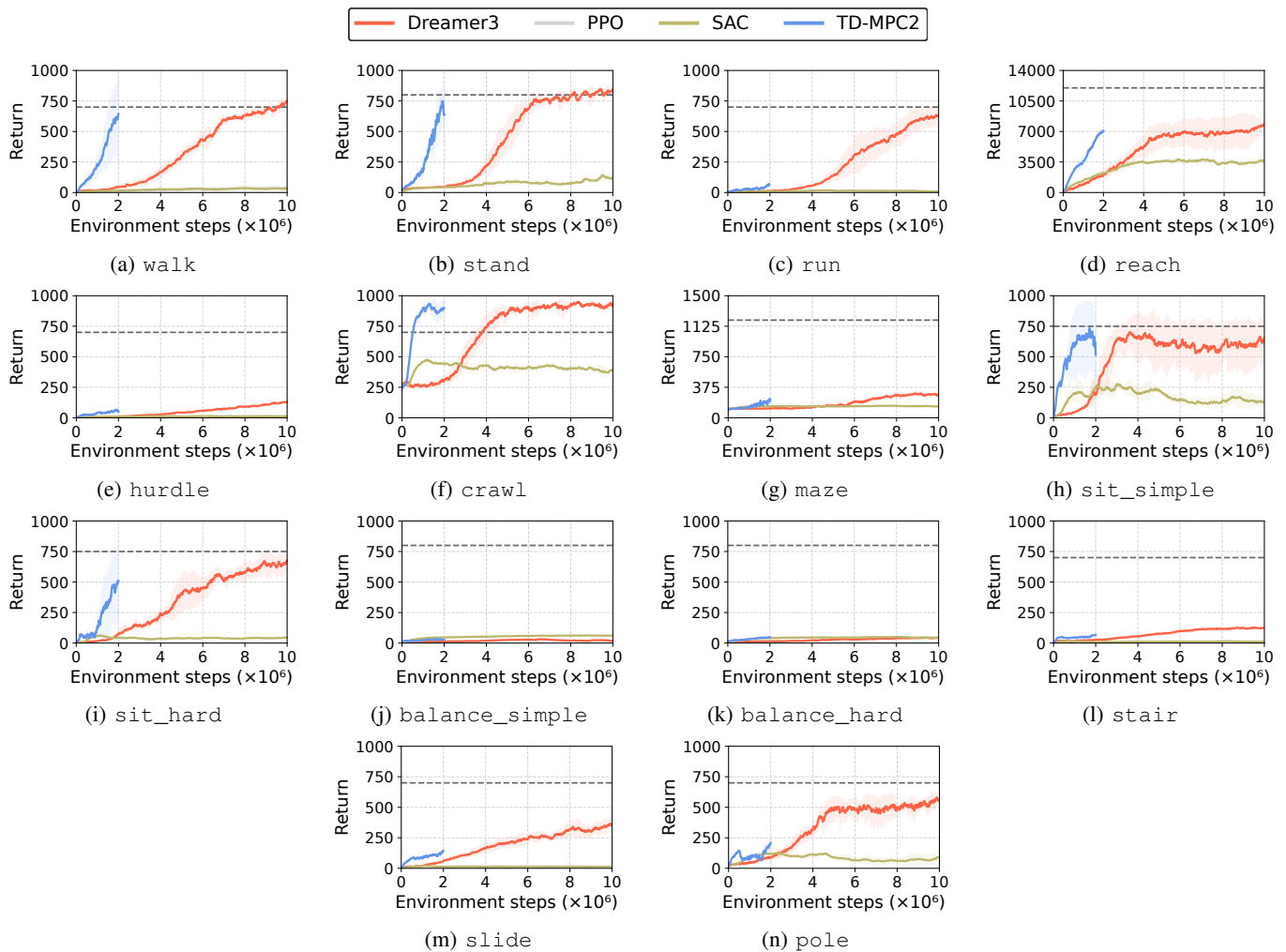


Fig. 5: **Learning curves of RL algorithms (locomotion).** The curves are averaged over three random seeds and the shaded regions represent the standard deviation. The dashed lines qualitatively indicate task success. We run PPO on the *walk* task but it is not visible in the plot since it only achieves very low returns.

on expert demonstrations, which are not only expensive but also challenging to collect for humanoid robots.

A. Baselines

We evaluate all tasks in our benchmark with four reinforcement learning methods (DreamerV3, TD-MPC2, SAC, PPO). Please refer to appendix, Section C, for implementation details.

- **DreamerV3** [17]: the state-of-the-art model-based RL algorithm, learning from imaginary model rollouts.
- **TD-MPC2** [18]: the state-of-the-art model-based RL algorithm with online planning.
- **SAC** (Soft Actor-Critic [15]): the state-of-the-art off-policy model-free RL algorithm.
- **PPO** (Proximal Policy Optimization [45]): the state-of-the-art on-policy model-free RL algorithm.

B. Results

We report benchmarking results in Figure 5 and Figure 6, where we ran each of the algorithms for approximately 48

hours, resulting in the visible differences in environment steps (e.g. 2M steps for TD-MPC2, 10M steps for DreamerV3). We only run PPO on a subset of tasks (*walk*, *kitchen*, *door*, *package*), given its inferior performance without massive parallelization. Each of the environments is evaluated with a combination of dense rewards and sparse subtask completion rewards, and for each of these we provide qualitative measures of task success (see dashed lines in Figure 5 and Figure 6).

All the baseline algorithms perform below the success threshold on most tasks, particularly struggling on tasks that require long-horizon planning and intricate whole-body coordination in a high-dimensional action space. Surprisingly, these state-of-the-art RL algorithms require a large number of steps to learn even simple locomotion tasks, such as *walk*, which has been extensively studied with a simplified humanoid agent in the DeepMind Control Suite [51].

This poor performance is mainly attributed to *the high-dimensionality of the state and action spaces* of our humanoid robot agent with dexterous hands. Although the hands of the

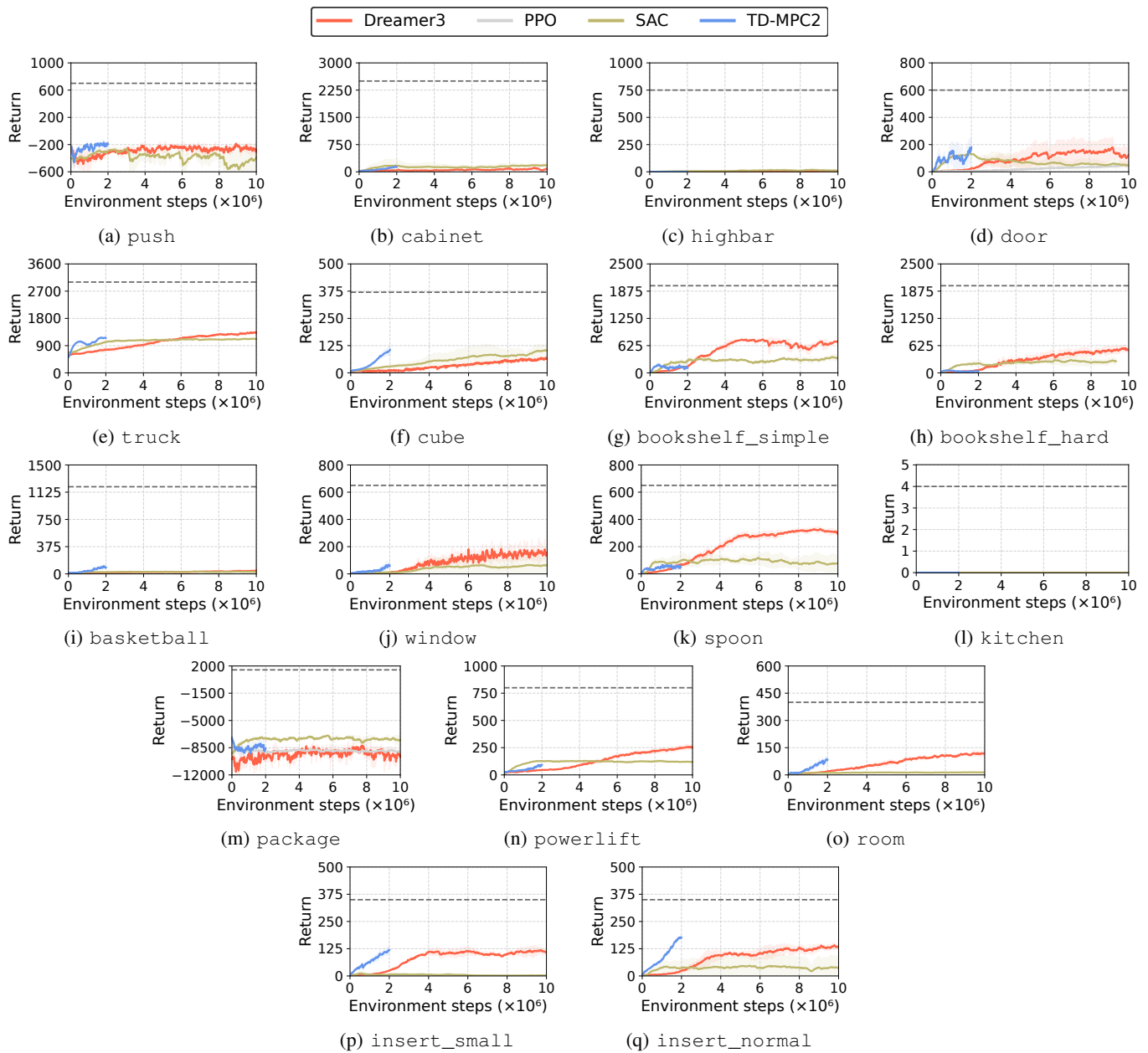


Fig. 6: **Learning curves of RL algorithms (manipulation).** The curves are averaged over three random seeds and the shaded regions represent the standard deviation. The dashed lines qualitatively indicate task success. Note that *kitchen* is the only environment with a purely discrete, sparse reward, with a maximum of 4.

humanoid robot are barely used for most locomotion tasks, the RL algorithms fail to ignore these information, which makes policy learning challenging. In addition, these high-dimensional state and action spaces result in a much larger exploration space, which makes exploration slow or infeasible with simple maximum entropy approaches. This implies the need for incorporating behavioral priors or common sense knowledge about the world that can ease the exploration problem, when it comes to learning more complex agents, like humanoid robots. We investigate this problem further in Section V-C.

This problem becomes even more severe in manipulation tasks, resulting in particularly low rewards in all manipulation tasks. Before learning any manipulation skills, an agent must learn locomotion skills to balance and move towards an object or the world to interact. All the policies barely learn to stabilize using the dense reward, but struggle to learn any complex manipulation skills.

C. With Hands vs. Without Hands

As discussed in Section V-B, controlling humanoid robots with dexterous hands is challenging due to their high degrees of freedom and complex dynamics. Thus, we investigate the

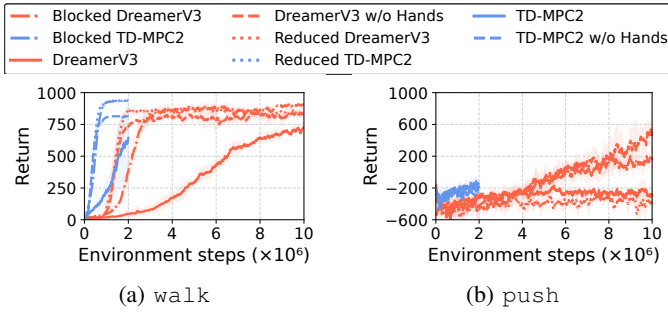


Fig. 7: **Performance with and without dexterous hands.** The curves are averaged over three random seeds and the shaded regions represent the standard deviation.

difficulty of RL training with a large action space (i.e. additional 42-DoFs with two dexterous Shadow Hands) on `walk` that does not necessarily require to control dexterous hands. The results in Figure 7 show that the presence of hands, with their additional joints and actuators, leads to a large decrease in performance compared to training the same task without the dexterous hands.

We perform an additional experiment to further confirm whether such difficulties stem from the dimensionality of the action space. In particular, we benchmark our full robot model, but fix the actuation of the hands, which we set to zero. In this way, the action dimensionality is reduced from 61 in the original model to 19, but the additional observations and masses induced by the presence of the hands are retained. On this experiment, the algorithms only slightly decrease their performance (see *Blocked* in the figure), confirming that most of the performance drop is indeed due to the increased action dimensionality. We repeat the same experiment, with similar results, by also removing the hand joints from the observation space (see *Reduced* in the figure). We observe similar trends in the more complex `push` task, which however, also presents substantially different dynamics in the task approach (e.g. pushing with and without hands).

D. Flat vs. Hierarchical Reinforcement Learning

As shown above, flat, end-to-end RL approaches fail to learn most of the tasks in HumanoidBench. The results above show that even state-of-the-art RL algorithms struggle on the most complex tasks in the benchmark. Many of such tasks require long-horizon planning and necessitate acquiring a diverse set of skills (e.g., balancing, walking, reaching, etc.) to successfully achieve the desired objective. We argue that these issues can be mitigated by introducing additional structure into the learning problem. In particular, we explore a hierarchical learning paradigm, where one or multiple low-level skill policies are provided to a high-level planning policy that sends setpoints to lower-level policies, see Figure 8. In practice, such setpoints comprise the action space of the high-level policy. This framework is very general, and there are no constraints on how to obtain both low-level and high-level policies. However, here we focus on training both of these

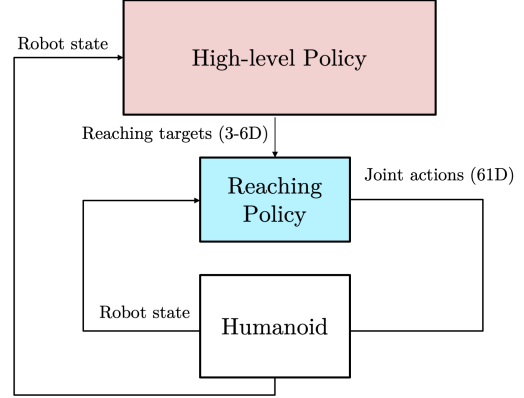


Fig. 8: Our hierarchical architecture, where a robust low-level reaching policy (trained using PPO) follows targets provided by a high-level planning policy.

through reinforcement learning.

We report results of such a hierarchical approach on two different tasks, namely, the `push` and `package` tasks. As a low-level skill, `push` uses a one-hand reaching policy, which allows the robot to reach a 3D point in space with its left hand, while `package` uses a two-hand reaching policy, where both hands are commanded to reach different 3D targets.

Ideally, the low-level skill policies are pretrained blocks that can be reused across tasks. In particular, our hierarchical architecture considers the low-level policy as a frozen block that does not improve during training of the high-level policy. As such, the low-level reaching policies in our `push` and `package` tasks need to be very robust to cope with the continually shifting reaching targets that the high-level policy sets during exploration. However, the results in the previous section show how even a one-hand reaching task is hard to learn for the algorithms benchmarked in this work.

On a separate note, while our experiments above confirm that the on-policy PPO exhibits poor sample efficiency compared to the other off-policy algorithms, it is worth noting that PPO has achieved significant success in robotic locomotion by exploiting large-scale parallelization of environments on GPUs [31]. We exploit hardware acceleration using the recently released MuJoCo MJX⁵, which enables training PPO on thousands of parallel environments. We employ a simplified H1 model that only considers collisions between feet and ground in our MJX experiments, as in our experience the advantages stemming from parallelization are largely reduced when considering all numerous humanoid geometries (hindering training of the more complex benchmark tasks via MJX). We also remove the hands from the model to further increase training efficiency. We modify the reaching task by resetting the target during each episode whenever this has been reached. We also apply force perturbations at each of the links during training. We train the one-hand reaching policy for 2 billion steps (36 hours) and

⁵<https://mujoco.readthedocs.io/en/stable/mjx.html>

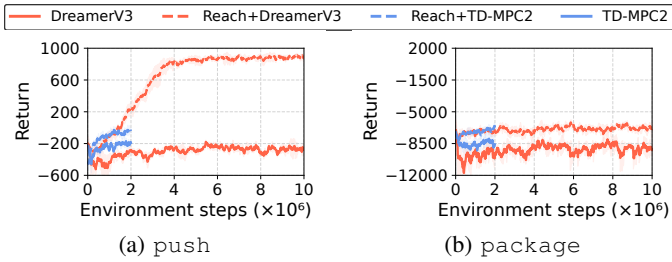


Fig. 9: **Comparison between flat policies and hierarchical policies.** The curves are averaged over three random seeds and the shaded regions represent the standard deviation.

the two-hand reaching policy for 4 billion steps (60 hours) on a total of 32,768 parallel environments. As a result of the robustness introduced by the force perturbations, our model directly transfers to the full humanoid model (with original collision meshes) on the classical MuJoCo simulation, and is also robust to the additional masses introduced by the presence of dexterous hands. We provide the MuJoCo MJX training code as part of our software package.

As mentioned above, we use the reaching policies obtained through MJX training as low-level policies of our hierarchical architecture. For the `push` and `package` tasks, we restrict the range of reaching targets to the robot workspace to facilitate exploration, and the high-level policies are trained with either DreamerV3 or TDMPC2. Results are shown in Figure 9, where the hierarchical architecture significantly outperforms the end-to-end baselines on the `push` task, achieving very high success rates. While the low-level policy has undergone additional pretraining, this can be in principle reused across tasks. We note a less pronounced performance improvement in the more challenging `package` task. While getting closer to picking up the package, the policy still struggles in lifting it (having never experienced it during training), which limits the overall task performance.

These results confirm that the tasks present in our benchmark present challenges that can be addressed with a more structured approach to the learning problem, and we hope this stimulates further directions for future research.

E. Common Failures

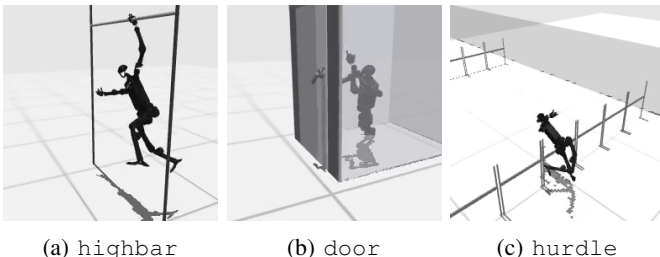


Fig. 10: **Failure Scenarios.** This figure presents a selection of common failures that occur while training our benchmark tasks.

In this subsection, we remark on notable challenges and common failures for some representative tasks in our benchmark, which denote the challenge in learning with high-dimensional action spaces and limited planning horizon of the state-of-the-art RL algorithms.

Common Failure on `highbar`. In the `highbar` task, the Unitree H1 robot conservatively learns to maintain contact with the bar to avoid episode termination, but experiences difficulties in performing the whole-body rotation trajectory. This is indicative of short horizon planning and, despite the availability of dense rewards, is a recurrent challenge in many of the long-horizon benchmark tasks.

Common Failure on `door`. In the `door` task, the robot is well-guided to turn the door hatch to unlock the door, but it finds it challenging to learn the precise motion required to pull the door towards its opening position. This is mainly because pulling the door requires not only pulling its arm but also moving the whole body backwards. The coordination between multiple body parts and seamless interaction between manipulation and locomotion skills are common challenges in training humanoid robots.

Common Failure on `hurdle`. In the `hurdle` environment, the robot learns to run forward with the expected velocity but does not recognize the need to surpass the hurdle by jumping, which is a hard exploration problem. Previous work has shown that in OpenAI gym Walker2d, the forward-moving reward is sufficient to learn this behavior [25]. On the other hand, the humanoid robot finds conservative poses to collide with the hurdle such that it can stabilize without terminating the episode after hitting the obstacle, without further exploring high-reward jumping behaviors.

VI. CONCLUSION

We presented HumanoidBench, a high-dimensional humanoid robot control benchmark. Ours is the first example of a comprehensive humanoid environment with a diversity of locomotion and manipulation tasks, ranging from toy examples to practical humanoid applications. We set a high bar with our complex tasks, in the hope to stimulate the community to accelerate the development of whole-body algorithms for such robotic platforms.

Future work. HumanoidBench already includes multi-modal high-dimensional observations in the form of egocentric vision and whole-body tactile sensing. While our experiments only benchmarked the performance of state-based environments, studying the interplay between different modalities is a compelling direction for future work.

Extensions of the humanoid environment will also eventually include more realistic objects and environments with real-world diversity and higher-quality rendering. As for dexterous manipulation tasks, we envision screwing and furniture assembly tasks being part of our framework, given that they are particularly tailored for bimanual manipulation.

Here we have focused on reinforcement learning algorithms because humanoids are a setting where collecting physical demonstrations may be challenging. However, we believe that

other means could be employed to bootstrap learning (e.g., learning from human videos).

Finally, while this was not the focus of our work, the impressive results obtained via domain randomization in the newly developed MuJoCo MJX show promise to study sim-to-real transfer in more depth, following the large success of the field in quadrupedal locomotion [20].

REFERENCES

- [1] Alphonsus Adu-Bredu, Grant Gibson, and Jessie Grizzle. Exploring kinodynamic fabrics for reactive whole-body control of underactuated humanoid robots. In *IEEE/RSJ International Conference on Intelligent Robots and Systems*, pages 10397–10404. IEEE, 2023.
- [2] Ilge Akkaya, Marcin Andrychowicz, Maciek Chociej, Mateusz Litwin, Bob McGrew, Arthur Petron, Alex Paino, Matthias Plappert, Glenn Powell, Raphael Ribas, et al. Solving rubik’s cube with a robot hand. *arXiv preprint arXiv:1910.07113*, 2019.
- [3] Firas Al-Hafez, Guoping Zhao, Jan Peters, and Davide Tateo. Locomujoco: A comprehensive imitation learning benchmark for locomotion. *6th Robot Learning Workshop at NeurIPS*, 2023.
- [4] M. G. Bellemare, Y. Naddaf, J. Veness, and M. Bowling. The arcade learning environment: An evaluation platform for general agents. *Journal of Artificial Intelligence Research*, 47:253–279, jun 2013.
- [5] Cameron H Berg, Vittorio Caggiano, and Vikash Kumar. SAR: Generalization of Physiological Dexterity via Synergistic Action Representation. In *Robotics: Science and Systems*, 2023.
- [6] Greg Brockman, Vicki Cheung, Ludwig Pettersson, Jonas Schneider, John Schulman, Jie Tang, and Wojciech Zaremba. Openai gym. *arXiv preprint arXiv:1606.01540*, 2016.
- [7] Vittorio Caggiano, Huawei Wang, Guillaume Durandau, Massimo Sartori, and Vikash Kumar. Myosuite: A contact-rich simulation suite for musculoskeletal motor control. In *Learning for Dynamics and Control*, pages 492–507. PMLR, 2022.
- [8] Vittorio Caggiano, Sudeep Dasari, and Vikash Kumar. Myodex: a generalizable prior for dexterous manipulation. In *International Conference on Machine Learning*, pages 3327–3346. PMLR, 2023.
- [9] Yuanpei Chen, Yiran Geng, Fangwei Zhong, Jiaming Ji, Jiechuang Jiang, Zongqing Lu, Hao Dong, and Yaodong Yang. Bi-dexhands: Towards human-level bimanual dexterous manipulation. *IEEE Transactions on Pattern Analysis and Machine Intelligence*, 2023.
- [10] Cheng Chi, Siyuan Feng, Yilun Du, Zhenjia Xu, Eric Cousineau, Benjamin Burchfiel, and Shuran Song. Diffusion policy: Visuomotor policy learning via action diffusion. In *Robotics: Science and Systems*, 2023.
- [11] Yan Duan, Marcin Andrychowicz, Bradly Stadie, Jonathan Ho, Jonas Schneider, Ilya Sutskever, Pieter Abbeel, and Wojciech Zaremba. One-shot imitation learning. In *Advances in Neural Information Processing Systems*, pages 1087–1098, 2017.
- [12] Zipeng Fu, Tony Z Zhao, and Chelsea Finn. Mobile aloha: Learning bimanual mobile manipulation with low-cost whole-body teleoperation. *arXiv preprint arXiv:2401.02117*, 2024.
- [13] Dibya Ghosh. dibyaghosh/jaxrl_m, 2023. URL https://github.com/dibyaghosh/jaxrl_m.
- [14] Abhishek Gupta, Vikash Kumar, Corey Lynch, Sergey Levine, and Karol Hausman. Relay policy learning: Solving long-horizon tasks via imitation and reinforcement learning. *Conference on Robot Learning*, 2019.
- [15] Tuomas Haarnoja, Aurick Zhou, Pieter Abbeel, and Sergey Levine. Soft actor-critic: Off-policy maximum entropy deep reinforcement learning with a stochastic actor. In *International Conference on Machine Learning*, pages 1856–1865, 2018.
- [16] Tuomas Haarnoja, Ben Moran, Guy Lever, Sandy H Huang, Dhruva Tirumala, Markus Wulfmeier, Jan Humpalik, Saran Tunyasuvunakool, Noah Y Siegel, Roland Hafner, Michael Bloesch, Kristian Hartikainen, Arunkumar Byravan, Leonard Hasenclever, Yuval Tassa, Fereshteh Sadeghi, Nathan Batchelor, Federico Casarini, Stefano Saliceti, Charles Game, Neil Sreendra, Kushal Patel, Marlon Gwira, Andrea Huber, Nicole Hurley, Francesco Nori, Raia Hadsell, and Nicolas Heess. Learning agile soccer skills for a bipedal robot with deep reinforcement learning. *arXiv preprint arXiv:2304.13653*, 2023.
- [17] Danijar Hafner, Jurgis Pasukonis, Jimmy Ba, and Timothy Lillicrap. Mastering diverse domains through world models. *arXiv preprint arXiv:2301.04104*, 2023.
- [18] Nicklas Hansen, Hao Su, and Xiaolong Wang. Td-mpc2: Scalable, robust world models for continuous control. In *International Conference on Learning Representations*, 2024.
- [19] Minh Heo, Youngwoon Lee, Doohyun Lee, and Joseph J. Lim. Furniturebench: Reproducible real-world benchmark for long-horizon complex manipulation. In *Robotics: Science and Systems*, 2023.
- [20] Jemin Hwangbo, Joonho Lee, Alexey Dosovitskiy, Dario Bellicoso, Vassilios Tsounis, Vladlen Koltun, and Marco Hutter. Learning agile and dynamic motor skills for legged robots. *Science Robotics*, 4(26):eaau5872, 2019.
- [21] Stephen James, Zicong Ma, David Rovick Arrojo, and Andrew J. Davison. Rlbench: The robot learning benchmark & learning environment. *IEEE Robotics and Automation Letters*, 2020.
- [22] Harini Kannan, Danijar Hafner, Chelsea Finn, and Dumitru Erhan. Robodesk: A multi-task reinforcement learning benchmark. <https://github.com/google-research/robodesk>, 2021.
- [23] Ashish Kumar, Zipeng Fu, Deepak Pathak, and Jitendra Malik. Rma: Rapid motor adaptation for legged robots. In *Robotics: Science and Systems*, 2021.
- [24] Seunghwan Lee, Moonseok Park, Kyoungmin Lee, and

- Jehee Lee. Scalable muscle-actuated human simulation and control. *ACM Transactions on Graphics*, 38(4):1–13, 2019.
- [25] Youngwoon Lee, Shao-Hua Sun, Sriram Somasundaram, Edward S. Hu, and Joseph J. Lim. Composing complex skills by learning transition policies. In *International Conference on Learning Representations*, 2019. URL <https://openreview.net/forum?id=rygrBhC5tQ>.
- [26] Youngwoon Lee, Jingyun Yang, and Joseph J. Lim. Learning to coordinate manipulation skills via skill behavior diversification. In *International Conference on Learning Representations*, 2020.
- [27] Youngwoon Lee, Edward S Hu, and Joseph J Lim. IKEA furniture assembly environment for long-horizon complex manipulation tasks. In *IEEE International Conference on Robotics and Automation*, 2021. URL <https://clvrai.com/furniture>.
- [28] Chengshu Li, Ruohan Zhang, Josiah Wong, Cem Gokmen, Sanjana Srivastava, Roberto Martín-Martín, Chen Wang, Gabrael Levine, Michael Lingelbach, Jiankai Sun, Mona Anvari, Minjune Hwang, Manasi Sharma, Arman Aydin, Dhruva Bansal, Samuel Hunter, Kyu-Young Kim, Alan Lou, Caleb R Matthews, Ivan Villa-Renteria, Jerry Huayang Tang, Claire Tang, Fei Xia, Silvio Savarese, Hyowon Gweon, Karen Liu, Jiajun Wu, and Li Fei-Fei. Behavior-1k: A benchmark for embodied ai with 1,000 everyday activities and realistic simulation. In *Conference on Robot Learning*, 2022.
- [29] Xingyu Lin, Yufei Wang, Jake Olkin, and David Held. Softgym: Benchmarking deep reinforcement learning for deformable object manipulation. In *Conference on Robot Learning*, 2020.
- [30] Chris Lu, Jakub Kuba, Alistair Letcher, Luke Metz, Christian Schroeder de Witt, and Jakob Foerster. Discovered policy optimisation. *Advances in Neural Information Processing Systems*, 35:16455–16468, 2022.
- [31] Viktor Makoviychuk, Lukasz Wawrzyniak, Yunrong Guo, Michelle Lu, Kier Storey, Miles Macklin, David Hoeller, Nikita Rudin, Arthur Allshire, Ankur Handa, and Gavriel State. Isaac gym: High performance gpu based physics simulation for robot learning. In *Neural Information Processing Systems Datasets and Benchmarks Track*, 2021.
- [32] Ajay Mandlekar, Danfei Xu, Josiah Wong, Soroush Nasiriany, Chen Wang, Rohun Kulkarni, Li Fei-Fei, Silvio Savarese, Yuke Zhu, and Roberto Martín-Martín. What matters in learning from offline human demonstrations for robot manipulation. In *Conference on Robot Learning*, 2021.
- [33] Dominik Mattern, Pierre Schumacher, Francisco M López, Marcel C Raabe, Markus R Ernst, Arthur Aubret, and Jochen Triesch. Mimo: A multi-modal infant model for studying cognitive development. *IEEE Transactions on Cognitive and Developmental Systems*, 2024.
- [34] Oier Mees, Lukas Hermann, Erick Rosete-Beas, and Wolfram Burgard. Calvin: A benchmark for language-conditioned policy learning for long-horizon robot manipulation tasks. *IEEE Robotics and Automation Letters*, 2022.
- [35] Josh Merel, Saran Tunyasuvunakool, Arun Ahuja, Yuval Tassa, Leonard Hasenclever, Vu Pham, Tom Erez, Greg Wayne, and Nicolas Heess. Catch & carry: reusable neural controllers for vision-guided whole-body tasks. *ACM Transactions on Graphics*, 39(4):39–1, 2020.
- [36] Philipp Mittendorf and Gordon Cheng. Humanoid multimodal tactile-sensing modules. *IEEE Transactions on robotics*, 27(3):401–410, 2011.
- [37] Yashraj Narang, Kier Storey, Iretiayo Akinola, Miles Macklin, Philipp Reist, Lukasz Wawrzyniak, Yunrong Guo, Adam Moravanszky, Gavriel State, Michelle Lu, Ankur Handa, and Dieter Fox. Factory: Fast contact for robotic assembly. In *Robotics: Science and Systems*, 2022.
- [38] OpenAI, Marcin Andrychowicz, Bowen Baker, Maciek Chociej, Rafal Jozefowicz, Bob McGrew, Jakub Pachocki, Arthur Petron, Matthias Plappert, Glenn Powell, Alex Ray, Jonas Schneider, Szymon Sidor, Josh Tobin, Peter Welinder, Lilian Weng, and Wojciech Zaremba. Learning dexterous in-hand manipulation. *The International Journal of Robotics Research*, 39(1):3–20, 2020.
- [39] Xue Bin Peng, Pieter Abbeel, Sergey Levine, and Michiel Van de Panne. Deepmimic: Example-guided deep reinforcement learning of physics-based character skills. *ACM Transactions on Graphics*, 37(4):1–14, 2018.
- [40] Xue Bin Peng, Angjoo Kanazawa, Jitendra Malik, Pieter Abbeel, and Sergey Levine. Sfv: Reinforcement learning of physical skills from videos. *ACM Transactions on Graphics*, 37(6):1–14, 2018.
- [41] Xue Bin Peng, Ze Ma, Pieter Abbeel, Sergey Levine, and Angjoo Kanazawa. Amp: Adversarial motion priors for stylized physics-based character control. *ACM Transactions on Graphics*, 40(4):1–20, 2021.
- [42] Matthias Plappert, Marcin Andrychowicz, Alex Ray, Bob McGrew, Bowen Baker, Glenn Powell, Jonas Schneider, Josh Tobin, Maciek Chociej, Peter Welinder, Vikash Kumar, and Wojciech Zaremba. Multi-goal reinforcement learning: Challenging robotics environments and request for research. *arXiv preprint arXiv:1802.09464*, 2018.
- [43] Ilija Radosavovic, Tete Xiao, Bike Zhang, Trevor Darrell, Jitendra Malik, and Koushil Sreenath. Learning humanoid locomotion with transformers. *arXiv preprint arXiv:2303.03381*, 2023.
- [44] Antonin Raffin, Ashley Hill, Maximilian Ernestus, Adam Gleave, Anssi Kanervisto, and Noah Dormann. Stable baselines3, 2019.
- [45] John Schulman, Filip Wolski, Prafulla Dhariwal, Alec Radford, and Oleg Klimov. Proximal policy optimization algorithms. *arXiv preprint arXiv:1707.06347*, 2017.
- [46] Carmelo Sferrazza and Raffaello D’Andrea. Sim-to-real for high-resolution optical tactile sensing: From images to three-dimensional contact force distributions. *Soft Robotics*, 9(5):926–937, 2022.
- [47] Carmelo Sferrazza, Younggyo Seo, Hao Liu, Young-

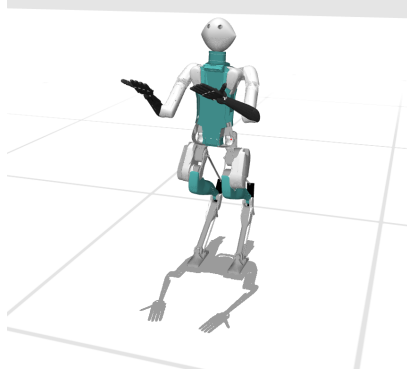
- woon Lee, and Pieter Abbeel. The power of the senses: Generalizable manipulation from vision and touch through masked multimodal learning. *arXiv preprint arXiv:2311.00924*, 2023.
- [48] Sanjana Srivastava, Chengshu Li, Michael Lingelbach, Roberto Martín-Martín, Fei Xia, Kent Elliott Vainio, Zheng Lian, Cem Gokmen, Shyamal Buch, Karen Liu, Silvio Savarese, Hyowon Gweon, Jiajun Wu, and Li Fei-Fei. Behavior: Benchmark for everyday household activities in virtual, interactive, and ecological environments. In *Conference on Robot Learning*, 2021.
- [49] Andrew Szot, Alex Clegg, Eric Undersander, Erik Wijmans, Yili Zhao, John Turner, Noah Maestre, Mustafa Mukadam, Devendra Chaplot, Oleksandr Maksymets, Aaron Gokaslan, Vladimir Vondrus, Sameer Dharur, Franziska Meier, Wojciech Galuba, Angel Chang, Zsolt Kira, Vladlen Koltun, Jitendra Malik, Manolis Savva, and Dhruv Batra. Habitat 2.0: Training home assistants to rearrange their habitat. In *Neural Information Processing Systems*, 2021.
- [50] Yuval Tassa, Yotam Doron, Alistair Muldal, Tom Erez, Yazhe Li, Diego de Las Casas, David Budden, Abbas Abdolmaleki, Josh Merel, Andrew LeFrancq, Timothy P. Lillicrap, and Martin A. Riedmiller. Deepmind control suite. *arXiv preprint arXiv:1801.00690*, 2018.
- [51] Yuval Tassa, Saran Tunyasuvunakool, Alistair Muldal, Yotam Doron, Siqi Liu, Steven Bohez, Josh Merel, Tom Erez, Timothy Lillicrap, and Nicolas Heess. dm_control: Software and tasks for continuous control. *arXiv preprint arXiv:2006.12983*, 2020.
- [52] Emanuel Todorov, Tom Erez, and Yuval Tassa. Mujoco: A physics engine for model-based control. In *IEEE/RSJ International Conference on Intelligent Robots and Systems*, pages 5026–5033, 2012.
- [53] Yinhuai Wang, Jing Lin, Ailing Zeng, Zhengyi Luo, Jian Zhang, and Lei Zhang. Physshoi: Physics-based imitation of dynamic human-object interaction. *arXiv preprint arXiv:2312.04393*, 2023.
- [54] Xinyue Wei, Minghua Liu, Zhan Ling, and Hao Su. Approximate convex decomposition for 3d meshes with collision-aware concavity and tree search. *ACM Transactions on Graphics (TOG)*, 41(4):1–18, 2022.
- [55] Zhaoming Xie, Jonathan Tseng, Sebastian Starke, Michiel van de Panne, and C Karen Liu. Hierarchical planning and control for box loco-manipulation. *Symposium on Computer Animation*, 2023.
- [56] Tianhe Yu, Deirdre Quillen, Zhanpeng He, Ryan Julian, Karol Hausman, Chelsea Finn, and Sergey Levine. Meta-world: A benchmark and evaluation for multi-task and meta reinforcement learning. In *Conference on Robot Learning*, 2019.
- [57] Ying Yuan, Haichuan Che, Yuzhe Qin, Binghao Huang, Zhao-Heng Yin, Kang-Won Lee, Yi Wu, Soo-Chul Lim, and Xiaolong Wang. Robot synesthesia: In-hand manipulation with visuotactile sensing. *arXiv preprint arXiv:2312.01853*, 2023.
- [58] Kevin Zakka, Yuval Tassa, and MuJoCo Menagerie Contributors. MuJoCo Menagerie: A collection of high-quality simulation models for MuJoCo, 2022. URL http://github.com/google-deepmind/mujoco_menagerie.
- [59] Kevin Zakka, Philipp Wu, Laura Smith, Nimrod Gileadi, Taylor Howell, Xue Bin Peng, Sumeet Singh, Yuval Tassa, Pete Florence, Andy Zeng, and Pieter Abbeel. Robopianist: Dexterous piano playing with deep reinforcement learning. In *Conference on Robot Learning*, pages 2975–2994. PMLR, 2023.
- [60] Haotian Zhang, Ye Yuan, Viktor Makoviychuk, Yunrong Guo, Sanja Fidler, Xue Bin Peng, and Kayvon Fatahalian. Learning physically simulated tennis skills from broadcast videos. *ACM Transactions on Graphics*, 42(4):1–14, 2023.
- [61] Tony Z Zhao, Vikash Kumar, Sergey Levine, and Chelsea Finn. Learning fine-grained bimanual manipulation with low-cost hardware. In *Robotics: Science and Systems*, 2023.
- [62] Yuke Zhu, Josiah Wong, Ajay Mandlekar, and Roberto Martín-Martín. robosuite: A modular simulation framework and benchmark for robot learning. *arXiv preprint arXiv:2009.12293*, 2020.
- [63] Ziwen Zhuang, Zipeng Fu, Jianren Wang, Christopher G Atkeson, Sören Schwertfeger, Chelsea Finn, and Hang Zhao. Robot parkour learning. In *Conference on Robot Learning*, 2023.

Appendix

Table of Contents

Appendix A: Additional Components	13
Appendix B: Simulated Environment Details	13
B-A Observation Space	13
B-B Action Space	13
B-C Simulation Performance	13
B-D Whole-body Tactile Sensing	13
B-E Task Specification	13
Appendix C: Training Details	22
C-A Baseline Implementation Details	22
C-B Reaching Policy Implementation Details	22
C-C Benchmarking Results	22

APPENDIX A ADDITIONAL COMPONENTS



In addition to the Unitree H1 robot, we also include model files for the Agility Robotics Digit humanoid. We add a custom head, together with egocentric vision and whole-body tactile sensing, similarly to the H1. We provide a torque controlled version of this robot.

We also provide two additional end effectors for the Unitree H1 robot, that is, a Robotiq 2F-45 parallel-jaw gripper, and a dexterous hand available in the Unitree model collection.

APPENDIX B SIMULATED ENVIRONMENT DETAILS

A. Observation Space

The observation space for the robot state (joint positions and velocities) comprises 151 dimensions, with 49 dimensions representing the humanoid robot body and 51 dimensions representing each hand. The observation space can also include environment states for tasks interacting with objects, as described in detail in Section B-E.

B. Action Space

The action space is the same across all environments. We normalize the action space to be $[-1, 1]^{\|A\|}$, where $\|A\| = 61$ (19 for the humanoid body and 21 for each hand). We use position control for the benchmarking results in this paper.

C. Simulation Performance

HumanoidBench is based on MuJoCo [52], which provides fast and accurate physics simulation. We provide a diverse set of configurations, such as the full humanoid model with two hands, the humanoid model without hands, and the humanoid model with collision meshes only on its feet. We use the fastest model (i.e. collision meshes only on feet) to train the low-level reaching policies, described in Section C-B.

We benchmark our HumanoidBench simulation using the Unitree H1 model and report its performance in Table II. Even with complex humanoid body and dexterous hands, HumanoidBench can run 1000+ FPS on a single CPU with a simulation timestep of 0.002 s.

Configuration	FPS
Without hands	2450
Simplified body collisions	3600
Collisions only for feet	5100
Default	1050

TABLE II: HumanoidBench Simulation Performance.

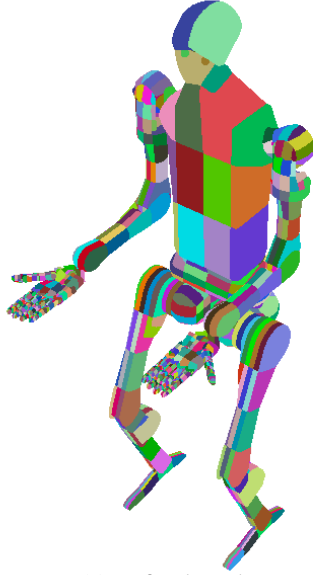
D. Whole-body Tactile Sensing

We implement whole-body tactile sensing by employing MuJoCo touch grid, which aggregates pressure and shear contact forces into discrete bins. Similar distributed force readings have been captured on real-world systems both on humanoid bodies [36] and end-effectors [46]. To increase the number of contact point candidates and fully exploit the spatial resolution of the touch grid, we subdivide the original meshes into many smaller meshes. Specifically, we build on top of CoACD [54], which in addition makes sure that the resulting meshes are all convex. This procedure results in finer contact resolution when the MuJoCo physics engine computes collisions. An example is depicted in Figure 11, with a larger number of contact points generally resulting in a considerably better discretization of the tactile readings. The full model with refined meshes and tactile readings runs at 550 FPS.

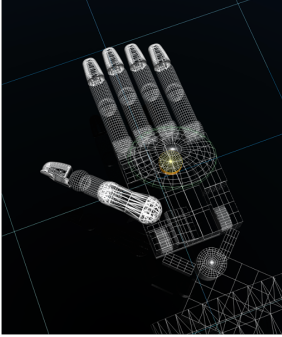
E. Task Specification

Before enumerating the environment details below, let us define auxiliary functions and variables that are employed in the reward functions of multiple environments:

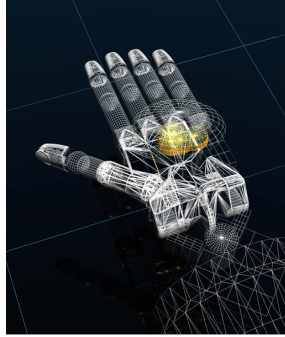
- $tol(x, (x_{lower}, x_{upper}), m)$ is a function provided in the DeepMind Control Suite package [51]. This is denoted there as a *tolerance* function that returns 1 when the evaluated value is within the bounds, i.e., $x \in (x_{lower}, x_{upper})$, and between 0 and 1 otherwise. The margin m regulates the slope of the function, i.e., how far from the bounds the function approaches 0.
- $height((x_{lower}, x_{upper}), m)$ is a variable defined as $tol(z_{head}, (x_{lower}, x_{upper}), m)$ that rewards the head height, where z_{head} is the vertical coordinate of the robot head position. Whenever the arguments are not indicated, we assume $x_{lower} = 1.65$, $x_{upper} = +\infty$, and $m = 0.4125$.



(a) Refined meshes



(b) Contact before refinement



(c) Contact after refinement

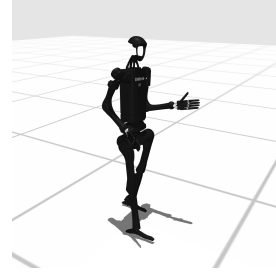
Fig. 11: **Refinement of collision meshes.** As a result of the mesh refinement (see (a), where each colored section indicates a different collision mesh), our model can detect a higher number of contact points, as shown by the yellow disks in the figure. This results in a better spatial discretization of the tactile readings.

- $d(\text{object}_A, \text{object}_B)$ is the distance between object A and object B.
- $\text{upright}((x_{\text{lower}}, x_{\text{upper}}), m)$ is a variable defined as $\text{tol}(z_{\text{proj}}, (x_{\text{lower}}, x_{\text{upper}}), m)$, which rewards the alignment of the robot torso with respect to the vertical axis, where z_{proj} is the unit projection of the z -axis in the robot body frame onto the z -axis in the global frame. Whenever the arguments are not indicated, we assume $x_{\text{lower}} = 0.9$, $x_{\text{upper}} = +\infty$, and $m = 1.9$.
- $\text{stand} := \text{height} \times \text{upright}$ represents a standing posture reward.
- $e := 0.2 \cdot \left[4 + \frac{1}{|u|} \sum_i \text{tol}(u_i, (0, 0), 10)\right]$ rewards small control effort, where u is the vector of actuation inputs.
- $\text{stable} = \text{stand} \times e$, densely rewards stable standing

configurations.

- v_x is the robot velocity in the x direction (positive forward) of the robot body coordinate frame.
- v_y is the robot velocity in the y direction (positive left) of the robot body coordinate frame.
- z_{item} is the vertical z coordinate of the indicated ‘item’ in the global frame.
- pos_{item} is the 3D position of the indicated ‘item’ in the global frame.

1) *walk*:



Objective. Keep forward velocity close to 1 m/s without falling to the ground.

Observation. Joint positions and velocities of the robot.

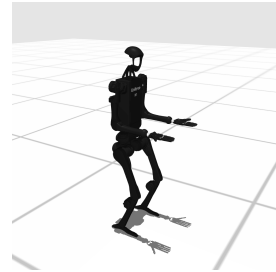
Initialization. The robot is initialized to a standing position, with random noise added to all joint positions during each episode reset.

Termination. The episode terminates after 1000 steps, or when $z_{\text{pelvis}} < 0.2$.

Reward Implementation.

$$R(s, a) = \text{stable} \times \text{tol}(v_x, (1, +\infty), 1).$$

2) *stand*:



Objective. Maintain a standing pose.

Observation. Joint positions and velocities of the robot.

Initialization. The robot is initialized to a standing position, with random noise added to all joint positions during each episode reset.

Reward Implementation. Let:

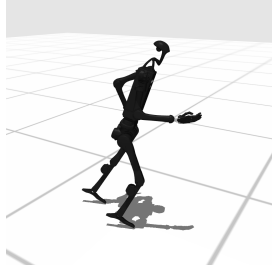
- $\text{still}_x = \text{tol}(v_x, (0, 0), 2)$
- $\text{still}_y = \text{tol}(v_y, (0, 0), 2)$,

Then:

$$R(s, a) = \text{stable} \times \text{mean}(\text{still}_x, \text{still}_y)$$

Termination. The episode terminates after 1000 steps, or when $z_{\text{pelvis}} < 0.2$.

3) *run*:



Objective. Keep forward velocity close to 5 m/s without falling to the ground.

Observation. Joint positions and velocities of the robot.

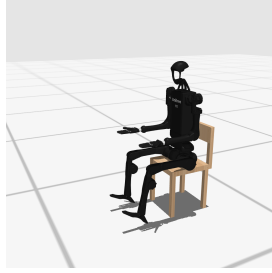
Initialization. The robot is initialized to a standing position, with random noise added to all joint positions during each episode reset.

Reward Implementation.

$$R(s, a) = \text{stable} \times \text{tol}(v_x, (5, \infty), 5)$$

Termination. The episode terminates after 1000 steps, or when $z_{\text{pelvis}} < 0.2$.

4) *sit*:



Objective. Sit onto a chair situated closely behind the robot.

Observation. In *sit_simple*, the observation is a vector containing all joint positions on the robot unit. In *sit_hard*, we allow the chair to be moved, and the robot initial position is randomized, so the observation includes position and orientation of the chair as well.

Initialization. The robot is initialized to a standing position, with random noise added to all joint positions during each episode reset. Note that in *sit_hard*, the robot is rotated at a random angle $\alpha \in [-1.8 \text{ rad}, 1.8 \text{ rad}]$ with position initialized at random values $x \in [0.2, 0.4]$, $y \in [-0.15, 0.15]$

Reward Implementation. Let

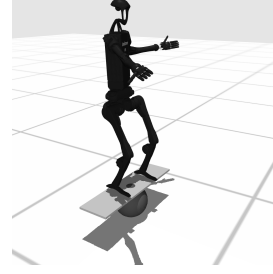
- $\text{sitting}_x = \text{tol}(x_{\text{robot}} - x_{\text{chair}}, (-0.19, 0.19), 0.2)$
- $\text{sitting}_y = \text{tol}(y_{\text{robot}} - y_{\text{chair}}, (0, 0), 0.1)$
- $\text{sitting}_z = \text{tol}(z_{\text{robot}}, (0.68, 0.72), 0.2)$
- $\text{posture} = \text{tol}(z_{\text{head}} - z_{\text{IMU}}, (0.35, 0.45), 0.3)$
- $\text{still}_x = \text{tol}(v_x, (0, 0), 2)$
- $\text{still}_y = \text{tol}(v_y, (0, 0), 2)$

then, the reward of this task is

$$R(s, a) = ((0.5 \cdot \text{sitting}_z + 0.5 \cdot \text{sitting}_x \times \text{sitting}_y) \times \text{upright} \times \text{posture}) \times e \times \text{mean}(\text{still}_x, \text{still}_y)$$

Termination. The episode terminates after 1000 steps, or when $z_{\text{pelvis}} < 0.5$.

5) *balance*:



Objective. Balance on the unstable board. There are two variants to this environment: the *balance_simple* variant's spherical pivot beneath the board does not move, while the *balance_hard* variant's pivot does.

Observation. The observation comprises the joint positions and velocities of the robot and those of the board.

Initialization. The robot is initialized to a standing position on the unstable board, with random noise added to all joint positions during each episode reset.

Reward Implementation. Let

- $\text{still}_x = \text{tol}(v_x, (0, 0), 2)$
- $\text{still}_y = \text{tol}(v_y, (0, 0), 2)$
- $\text{still} = \frac{1}{2}(\text{still}_x + \text{still}_y)$
- $\text{height}_{\text{robot}} = \text{height}((2.15, +\infty))$

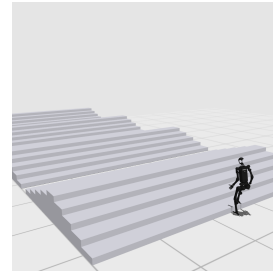
Then:

$$R(s, a) = (e \times \text{still}) \times (\text{height}_{\text{robot}} \times \text{upright})$$

Termination. The episode terminates after 1000 steps, or when one of the following condition satisfies:

- $z_{\text{robot}} < 0.8$
- The sphere collides with anything other than the floor and the standing board.
- The standing board collides with the floor.

6) *stair*:



Objective. Traverse an iterating sequence of upward and downward stairs at 1 m/s.

Observation. Joint positions and velocities of the robot.

Initialization. The robot is initialized to a standing position, with random noise added to all joint positions during each episode reset.

Reward Implementation. Let

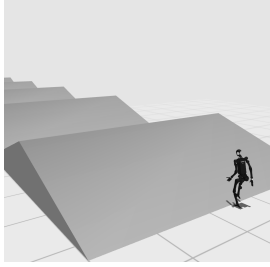
- $\text{vertical}_{\text{foot, left}} = \text{tol}(z_{\text{head}} - z_{\text{foot, left}}, (1.2, +\infty), 0.45)$
- $\text{vertical}_{\text{foot, right}} = \text{tol}(z_{\text{head}} - z_{\text{foot, right}}, (1.2, +\infty), 0.45)$

Then:

$$R(s, a) = e \times \text{tol}(v_x, (1, +\infty), 1) \times \text{upright}((0.5, 1), 1.9) \\ \times (\text{vertical}_{\text{foot, left}} \times \text{vertical}_{\text{foot, right}})$$

Termination. The episode terminates after 1000 steps, or when $z_{\text{proj}} < 0.1$.

7) *slide*:



Objective. Walk over an iterating sequence of upward and downward slides at 1 m/s.

Observation. Joint positions and velocities of the robot.

Initialization. The robot is initialized to a standing position, with random noise added to all joint positions during each episode reset.

Reward Implementation. Let

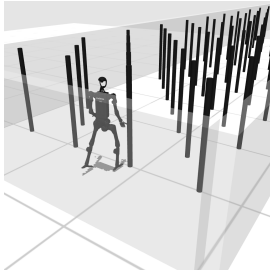
- $\text{vertical}_{\text{foot, left}} = \text{tol}(z_{\text{head}} - z_{\text{foot, left}}, (1.2, +\infty), 0.45)$
- $\text{vertical}_{\text{foot, right}} = \text{tol}(z_{\text{head}} - z_{\text{foot, right}}, (1.2, +\infty), 0.45)$

Then:

$$R(s, a) = e \times \text{tol}(v_x, (1, +\infty), 1) \times \text{upright}((0.5, 1), 1.9) \\ \times (\text{vertical}_{\text{foot, left}} \times \text{vertical}_{\text{foot, right}})$$

Termination. The episode terminates after 1000 steps, or when $z_{\text{proj}} < 0.6$.

8) *pole*:



Objective. Travel in forward direction over a dense forest of high thin poles, without colliding with them.

Observation. Joint positions and velocities of the robot.

Initialization. The robot is initialized to a standing position, with random noise added to all joint positions during each episode reset.

Reward Implementation. Let

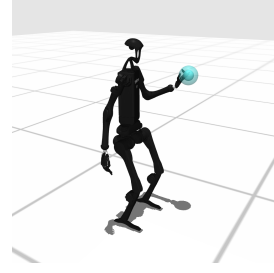
- $\gamma_{\text{collision}} = \begin{cases} 0.1, & \text{robot collides with pole} \\ 1, & \text{otherwise} \end{cases}$

Then,

$$R(s, a) = \gamma_{\text{collision}} \times (0.5 \cdot \text{stable} + 0.5 \cdot \text{tol}(v_x, (1, +\infty), 1)).$$

Termination. The episode terminates after 1000 steps, or when $z_{\text{pelvis}} < 0.6$.

9) *reach*:



Objective. Reach a randomly initialized 3D point with the left hand.

Observation. Joint positions and velocities of the robot, left hand position of robot, and reaching target position.

Initialization. The robot is initialized to a standing position, with random noise added to all joint positions during each episode reset.

Reward Implementation. Let

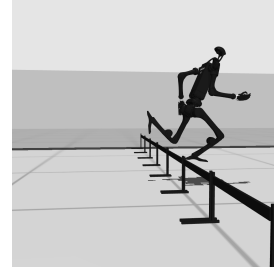
- $d_{\text{hand}} = d(\text{hand}_{\text{left}}, \text{goal})$
- $\text{health} = 5 \cdot z_{\text{pelvis, proj}}$
- $\text{penalty}_{\text{motion}} = \|v_{\text{robot}}\|^2$
- $\text{close} = \begin{cases} 5, & d_{\text{hand}} < 1 \\ 0, & \text{otherwise} \end{cases}$
- $\text{success} = \begin{cases} 10, & d_{\text{hand}} < 0.05 \\ 0, & \text{otherwise} \end{cases}$

Then,

$$R(s, a) = -10^{-4} \cdot \text{penalty}_{\text{motion}} + \text{health} + \text{close} + \text{success}$$

Termination. The episode terminates after 1000 steps.

10) *hurdle*:



Objective. Keep forward velocity close to 5 m/s without falling to the ground.

Observation. Joint positions and velocities of the robot.

Initialization. The robot is initialized to a standing position, with random noise added to all joint positions during each episode reset.

Reward Implementation. Let

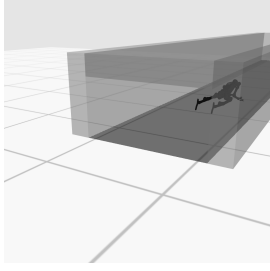
$$\gamma_{\text{collision}} = \begin{cases} 0.1 & \text{robot is colliding with wall} \\ 1 & \text{otherwise} \end{cases}$$

Then, we formulate the reward of this task as:

$$R(s, a) = \text{stable} \times \text{tol}(v_x, (5, \infty), 5) \times \gamma_{\text{collision}}$$

Termination. The episode terminates after 1000 steps.

11) *crawl*:



Objective. Keep forward velocity close to 1 m/s while passing inside a tunnel.

Observation. Joint positions and velocities of the robot.

Initialization. The robot is initialized to a standing position, with random noise added to all joint positions during each episode reset.

Reward Implementation. Let:

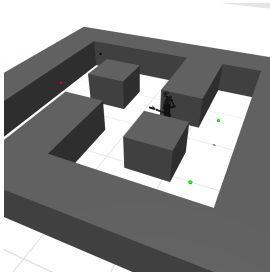
- $height_{crawl} = height((0.6, 1), 1)$
- $height_{IMU} = tol(z_{IMU}, (0.6, 1), 1)$
- $quat_{crawl} = [0.75 \ 0 \ 0.65 \ 0]$ is the expected quaternion expected when the robot is crawling.
- $orientation = tol(\|quat_{pelvis} - quat_{crawl}\|, (0, 0), 1)$ rewards correct robot body orientation.
- $tunnel = tol(y_{IMU}, (-1, 1), 0)$ rewards the robot when its y coordinate is inside the tunnel.
- $speed = tol(v_x, (1, +\infty), 1)$

Then, the reward is formulated as:

$$R = tunnel \times (0.1 \cdot e + 0.25 \cdot \min(height_{crawl}, height_{IMU}) + 0.25 \cdot orientation + 0.4 \cdot speed)$$

Termination. The episode terminates after 1000 steps.

12) *maze*:



Objective. Reach the goal position in a maze by taking multiple turns at the intersections.

Observation. Joint positions and velocities of the robot.

Initialization. The robot is initialized to a standing position, with random noise added to all joint positions during each episode reset.

Reward Implementation. For each checkpoint in the maze, we assign v_{target} to be the velocity prescribed to travel from the previous checkpoint towards next one. Then, let

- $move =$

$$tol(v_x - v_{target_x}, (0, 0), v_{target_x}) \times tol(v_y - v_{target_y}, (0, 0), v_{target_y})$$

- $\gamma_{collision} = \begin{cases} 0.1 & , \text{robot is colliding with wall} \\ 1 & , \text{otherwise} \end{cases}$
- $proximity = tol(d(checkpoint, pos_{robot}), (0, 0), 1)$

We formulate the reward as

$$R(s, a) = (0.2 \cdot stable + 0.4 \cdot move + 0.4 \cdot proximity) \times \gamma_{collision}$$

We also provide a sparse reward of $i \times 100$ for arriving at the i^{th} checkpoint.

Termination. The episode terminates after 1000 steps, or when $z_{pelvis} < 0.2$.

13) *push*:



Objective. Move a box to a randomly initialized 3D point on a table.

Observation. Joint positions and velocities of the robot, left hand position of the robot, box destination, box position, and box velocity.

Initialization. The robot is initialized to a standing position. The box and its destination are initialized at a random location on the table. Random noise is added to all joint positions during each episode reset.

Reward Implementation. Let:

- $d_{goal} = d(box, destination)$
- $success = \mathbb{1}_{d_{goal} < 0.05}$
- $d_{hand} = d(box, hand_{left})$

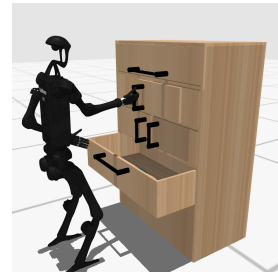
Then the reward is

$$R(s, a) = \alpha_s \cdot success - \alpha_t \cdot d_{goal} - \alpha_h \cdot d_{hand}$$

where by default $\alpha_s = 1000, \alpha_t = 1, \alpha_h = 0.1$.

Termination. The episode terminates after 500 steps, or when $d_{goal} < 0.05$.

14) *cabinets*:



Objective. Open four different types of cabinet doors (e.g. hinge door, sliding door, drawer) and perform different manipulations (see subtasks below) for objects inside the cabinet.

Observation. Positions and velocities of the robot’s joints, the cabinets’ joints, and the objects situated inside the cabinets.

Initialization. The robot is initialized to a standing position, with random noise added to all joint positions during each episode reset.

Reward Implementation. The reward of this task changes based on the occurring subtask.

Subtask 1 is to open the sliding door (second highest one), with reward

$$R_1 = 0.2 \cdot stable + 0.8 \cdot |l_{cabinet}/0.4|$$

where the cabinet joint position $l_{cabinet}$ is a value in $[0, 0.4]$.

Subtask 2 is to open the drawer (the lowest one), with reward

$$R_2 = 0.2 \cdot stable + 0.8 \cdot |l_{drawer}/0.45|$$

where the drawer joint position l_{drawer} is a value in $[0, 0.45]$.

Subtask 3 is to put the cube from the drawer into the hinge-based cabinet (the third highest one). Both the left and right hinge-based cabinet doors’ joint positions $\alpha_{door,left}$, $\alpha_{door,right}$ are values in $[0, 1.57]$. Let

- $open_{door,left} = \min(1, |\alpha_{door,left}|)$
- $open_{door,right} = \min(1, |\alpha_{door,right}|)$
- $d_{destination,x} = tol(x_{cube} - 0.9, (-0.3, 0.3), 0.3)$
- $d_{destination,y} = tol(y_{cube}, (-0.6, 0.6), 0.3)$
- $d_{destination,z} = tol(z_{cube} - 0.94, (-0.15, 0.15), 0.3)$
- $r_{destination} = 0.3 \cdot mean(d_{destination,x}, d_{destination,y}) + 0.7 \cdot d_{destination,z}$

Then the reward of this subtask, R_3 , is formulated as follows

$$r_3 = 0.5 \cdot \max(open_{door,left}, open_{door,right}) + 0.5 \cdot r_{destination}$$

$$R_3 = 0.2 \cdot stable + 0.8 \cdot r_3$$

Subtask 4 is to put the original cube from the hinge-based left-right cabinet (third highest) into the pull-up cabinet (highest). The pull-up door has a joint position α_{pull} in $[0, 1.57]$. Let

- $open_{pull} = \min(1, |\alpha_{pull}|)$
- $d_{destination,x} = tol(x_{cube} - 0.9, (-0.3, 0.3), 0.3)$
- $d_{destination,y} = tol(y_{cube}, (-0.6, 0.6), 0.3)$
- $d_{destination,z} = tol(z_{cube} - 1.54, (-0.15, 0.15), 0.3)$
- $r_{destination} = 0.3 \cdot mean(d_{destination,x}, d_{destination,y}) + 0.7 \cdot d_{destination,z}$

Then the reward of this subtask, R_4 , is formulated as follows

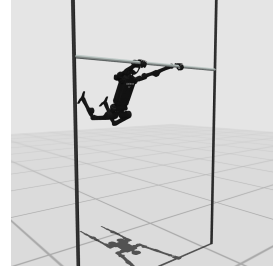
$$r_4 = 0.5 \cdot open_{pull} + 0.5 \cdot r_{destination}$$

$$R_4 = 0.2 \cdot stable + 0.8 \cdot r_4$$

The reward during the occurrence of subtask i is R_i . Upon the completion of subtask i , a sparse reward of $i * 100$ is offered. At the timestep where all subtasks are completed, a sparse reward of 1000 is added to the total reward.

Termination. The episode terminates after 1000 steps or whenever all subtasks are complete.

15) *highbar*:



Objective. Athletically swing while staying attached to a horizontal high bar until reaching a vertical upside-down position.

Observation. Joint positions and velocities of the robot.

Initialization. The robot is initialized such that its hand is gripping the high bar, and its body is hanging from it.

Reward Implementation. Let

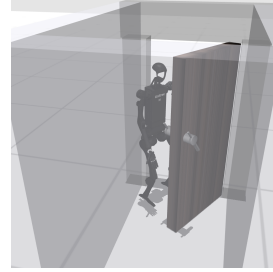
- $upright_{highbar} = upright((-\infty, -0.9), 1.9)$
- $feet = tol((z_{foot,left} + z_{foot,right})/2, (4.8, +\infty), 2)$

Then,

$$R(s, a) = upright_{highbar} \times feet \times e$$

Termination. The episode terminates after 1000 steps, or when $z_{head} < 2$.

16) *door*:



Objective. Pull a door open using its doorknob, and traverse through the doorpath while keeping the door open.

Observation. Joint positions and velocities of the robot, door hinge, and door hatch.

Initialization. The robot is initialized to a standing position. The door hinge joint and door latch are initialized such that the door is completely closed. For the current implementation, the door can only be pulled towards the robot, limiting its hinge joint position to be within $[0, 1.4]$. The door latch has a joint range of $[0, 2]$ (being pulled downwards until 2 radians from positive x-axis, clockwise). Random noise is added to all joint positions during each episode reset.

Reward Implementation. Let

- $open_{door} = \min(1, q_{door}^2)$
- $open_{hatch} = tol(q_{hatch}, (0.75, 2), 0.75)$
- $proximity_{door} =$

$$tol(\min(d(hand_{left}, door), d(hand_{right}, door)), (0, 0.25), 1)$$

- $passage = tol(x_{IMU}, (1.2, +\infty), 1)$

Then, the reward of this task is:

$$R = 0.1 \cdot stable + 0.45 \cdot open_{door} + 0.05 \cdot open_{hatch} + 0.05 \cdot proximity_{door} + 0.35 \cdot passage$$

Termination. The episode terminates after 1000 steps, or when $z_{pelvis} < 0.58$.

17) *truck*:



Objective. Unload packages from a truck by moving them onto a platform.

Observation. Joint positions and velocities of the robot, and positions and velocities of packages.

Initialization. The robot is initialized to a standing position. Packages are initialized to be on the truck. Random noise is added to all joint positions during each episode reset.

Reward Implementation. The reward of this task relies on the subsets of packages based on three categories: (1) being on truck (p_{truck}), (2) being picked up (p_{picked}), and (3) being on table (p_{table}). Let

- $truck = tol(\min_{p \in p_{truck}} \|pos_p - pos_{pelvis}\|, (0, 0.2), 4)$
- $picked = tol(\min_{p \in p_{picked}} \|pos_p - pos_{pelvis}\|, (0, 0.2), 4)$
- $table = tol(\min_{p \in p_{table}} \|pos_p - pos_{table}\|, (0, 0.2), 4)$
- $r_{location} = 100 \cdot (p_{table} + p_{picked} - p_{truck})$

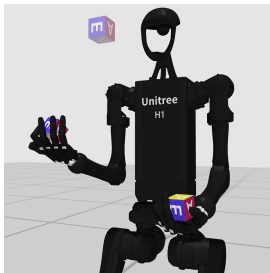
Then, the reward is:

$$R(s, a) = r_{location} + upright \times (1 + truck + picked + table)$$

If all packages are picked up, an additional sparse reward of 1000 is provided, and the episode terminates thereafter.

Termination. The episode terminates after 1000 steps, or when all packages are delivered onto the table.

18) *cube*:



Objective. Manipulate two cubes, each cube in one hand, until they both correspond with a specific, randomly initialized target orientation.

Observation. Joint positions and velocities of the robot and the two cubes to be manipulated on hand. The transparent cube

in front of the robot is an indication of the target orientation for in-hand cubes, and its orientation is also in the state.

Initialization. The robot is initialized to a standing position. The cubes are initialized at a random orientation right above the robot hands. Random noise is added to all joint positions during each episode reset.

Reward Implementation. Let

- $still_x = tol(v_x, (0, 0), 2)$
- $still_y = tol(v_y, (0, 0), 2)$
- $still = mean(still_x, still_y)$
- $quat_{target}$ denotes the target orientation for both in-hand cubes.
- $orientation = \frac{1}{2} [(quat_{cube, left} - quat_{target})^2 + (quat_{cube, right} - quat_{target})^2]$
- $proximity_{cube} =$

$$\frac{1}{2} [tol(d(cube_{left}, hand_{left}), (0, 0), 0.5) + tol(d(cube_{right}, hand_{right}), (0, 0), 0.5)]$$

Then the reward of this task is:

$$R = 0.2 \cdot (stable \times still) + 0.5 \cdot orientation + 0.3 \cdot proximity_{cube}$$

Termination. The episode terminates after 500 steps, or when $z_{pelvis} < 0.5$, $z_{cube, left} < 0.5$, or $z_{cube, right} < 0.5$.

19) *bookshelf*:



Objective. The bookshelf environment mainly concerns relocating five objects across the various shelves. There are five designated subtasks, resembling five different relocations (each for a different item and destination location). The items involved in the subtasks are colored from brightest to darkest in a red shade, where the brighter shade of red shows that the object's relocation is an earlier subtask to complete. The subtasks must be completed in order. The order is always the same in *bookshelf_simple*, while it is randomized at every episode in *bookshelf_hard*.

Observation. Positions and velocities of the robot's joints and all objects on the bookshelf, including those that are not associated with any subtasks, as well as an index representing the next object to be relocated.

Initialization. The robot is initialized to a standing position. All objects on the bookshelf are currently initialized at a default position. Random noise is added to all joint positions during each episode reset. In the simple version of this environment, the objects to move on the bookshelf and their destinations are

fixed; in the hard version, both of them are randomized at the beginning of every episode instead.

Reward Implementation. For each subtask t_i where $i \in \{1, 2, \dots, 5\}$, its reward r_i is formulated as follows. First, let

- $proximity_{destination} = tol(d(object, destination), (0, 0.15), 1)$
- $d_{hand} = \min(d(object, hand_{left}), d(object, hand_{right}))$
- $proximity_{hand} = \exp(-d_{hand})$.

Then, the subtask reward is

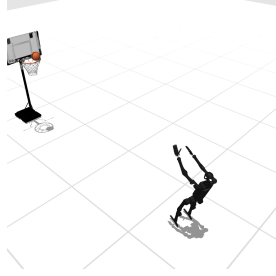
$$r_i = 0.4 \cdot proximity_{hand} + 0.2 \cdot stable + 0.4 \cdot proximity_{destination}$$

and the reward for that step is the subtask reward per se. The current subtask is considered complete when the distance between the destination and object of current subtask is less than 0.15.

An additional sparse reward of $100 * i$ is added to the timestep of subtask i 's completion.

Termination. The episode terminates after 1000 steps, or when $z_{pelvis} < 0.58$, $z_{object} < 0.5$, or all subtasks succeeded.

20) *basketball*:



Objective. Catch a ball coming from random direction and throw it into the basket.

Observation. Positions and velocities of the robot's joints and the basketball.

Initialization. The robot is initialized to a standing position. The basketball is initialized such that it will be randomly spawned at a radius of 1.5 m from the robot, at a random angle $\omega \in [-1.45 \text{ rad}, 1.45 \text{ rad}]$ from positive x-axis, and arrive right in front of the robot after 0.2 s. Random noise is added to all joint positions during each episode reset.

Reward Implementation. The task is divided into two stages:

- catch : before the basketball collides with anything
- throw : after the basketball experiences one collision

The rewards at different stages are formulated differently. Let

- $proximity_{hand} = tol(\max(d(ball, hand_{left}), d(ball, hand_{right})), (0, 0.2), 1)$
- $aim = tol(d(ball, basket), (0, 0), 7)$.

Then, the reward at each stage of the task is formulated as follows:

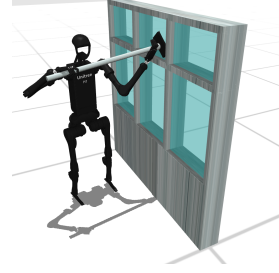
$$R_{catch}(x, u) = 0.5 \cdot proximity_{hand} + 0.5 \cdot stable$$

$$R_{throw}(x, u) = 0.05 \cdot proximity_{hand} + 0.15 \cdot stable + 0.8 \cdot aim$$

At the earliest timestep where $d(ball, basket) \leq 0.05$, the episode terminates, and a large sparse reward of 1000 is given.

Termination. The episode terminates after 500 steps, or when $z_{pelvis} < 0.5$, $z_{ball} < 0.5$, or when success has been achieved.

21) *window*:



Objective. Grab a window wiping tool and keep its tip parallel to a window by following a prescribed vertical speed (in absolute value).

Observation. Joint positions and velocities of the robot and the window wiping tool (position and velocities of the entire tool, in addition to those of the rotational joint attached between the wipe and the rod of the tool).

Initialization. The robot is initialized to a standing position. The window wiping tool is initialized above the robot unit's hand in a parallel direction to the window frames. Random noise is added to all joint positions during each episode reset.

Reward Implementation. Let

- $proximity_{tool} = \frac{1}{2} [tol(d(tool, hand_{left}), (0, 0), 0.5) + tol(d(tool, hand_{right}), (0, 0), 0.5)]$
- $d_{window} = tol(d(head, window), (0.4, 0.4), 0.1)$
- $move_{wipe} = tol(|v_{wipe,z}|, (0.5, 0.5), 0.5)$

The manipulation reward is defined as:

$$r_{manipulation} = 0.4 \cdot move_{wipe} + 0.4 \cdot proximity_{tool} + 0.2 \cdot (stable \times d_{window})$$

Meanwhile, five sites are put on the four corners and center of the wipe to detect coverage of contact. Let these sites be s_1, s_2, \dots, s_5 , then the reward for contact between the tool and window is defined as:

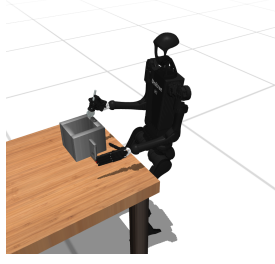
$$r_{contact} = \frac{1}{5} \sum_{s_i} tol(x_{s_i}, (0.92, 0.92), 0.4)$$

Then, the reward of this task is:

$$R = 0.5 \cdot r_{manipulation} + 0.5 \cdot r_{contact}$$

Termination. The episode terminates after 1000 steps, or when $z_{pelvis} < 0.58$ or $z_{tool} < 0.58$.

22) *spoon*:



Objective. Grab a spoon and use it to follow a circular pattern inside a pot.

Observation. Joint positions and velocities of the robot and the position and velocity of the spoon, as well as the target position that the spoon should be at the current timestep.

Initialization. The robot is initialized to a standing position. The spoon is initialized at a specified position on the table, leftwards of the pot. Random noise is added to all joint positions during each episode reset.

Reward Implementation. Let

- $t :=$ current timestep
- $proximity_{tool} =$

$$\frac{1}{2} [tol(d(tool, hand_{left}), (0, 0), 0.5) + tol((tool, hand_{right}), (0, 0), 0.5)]$$

- $destination = \begin{bmatrix} x_{pot} + 0.06 \cos(\frac{t\pi}{20}) \\ y_{pot} + 0.06 \sin(\frac{t\pi}{20}) \\ z_{pot} \end{bmatrix}$
- $r_{trajectory} = tol(d(spoon, destination), (0, 0), 0.15)$
- $r_{destination} = \frac{1}{3} \sum_{i \in \{x, y, z\}} \mathbb{1}_{i_{spoon \text{ in the pot}}}$

Then:

$$R(s, a) = 0.15 \cdot stable + 0.25 \cdot proximity_{tool} + 0.25 \cdot r_{destination} + 0.35 \cdot r_{trajectory}$$

Termination. The episode terminates after 1000 steps, or when $z_{pelvis} < 0.58$.

23) *kitchen*:



Objective. Execute a sequence of actions in a kitchen environment, namely, open a microwave door, move a kettle, and turn burner and light switches.

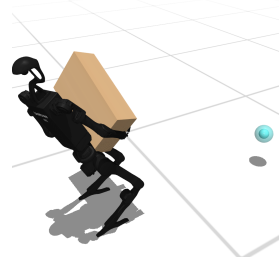
Observation. Joint positions and velocities of the robot, and positions and velocities of kitchenware.

Initialization. The robot is initialized to a standing position. Kitchenware is initialized at specified positions. Random noise is added to all joint positions during each episode reset.

Reward Implementation. A subtask in *kitchen* is considered complete if the distance between an object and its goal position is lower than a specified threshold. The sparse reward is the number of subtasks completed.

Termination. The episode terminates after 500 steps.

24) *package*:



Objective. Move a box to a randomly initialized target position, also tested in the ablation in Figure 9.

Observation. Joint positions and velocities of the robot, both hand positions of the robot, package destination, package position, and package velocity.

Initialization. The robot is initialized to a standing position. The package position and its destination are randomly initialized within a specific area. Random noise is added to all joint positions during each episode reset.

Reward Implementation. Let

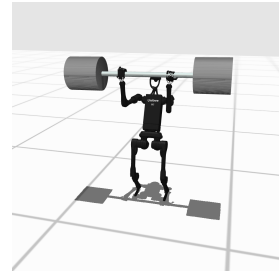
- $height_{package} = \min(1, z_{package})$
- $success = \mathbb{1}_{d(package, destination) < 0.1}$
- $d_{hand} = d(package, hand_{left}) + d(package, hand_{right})$.

Then, the reward is:

$$R(s, a) = -3 \cdot d(package, destination) - 0.1 \cdot d_{hand} + stable + height_{package} + 1000 \cdot success$$

Termination. The episode terminates after 1000 steps, or when $d(package, destination) < 0.1$.

25) *powerlift*:



Objective. Lift a barbell of a designated mass.

Observation. Joint positions and velocities of the robot and barbell.

Initialization. The robot is initialized to a standing position. The barbell is initialized on the ground. Random noise is added to all joint positions during each episode reset.

Reward Implementation. Let

- $height_{barbell} = tol(z_{barbell}, (1.9, 2.1), 2)$.

Then,

$$R(s, a) = 0.2 \cdot stable + 0.8 \cdot height_{barbell}.$$

Termination. The episode terminates after 1000 steps, or when $z_{pelvis} < 0.2$.

26) *room*:



Objective. Organize a 5 m by 5 m space populated with randomly scattered object to minimize the variance of scattered objects’ locations in x, y -axis directions.

Observation. Joint positions and velocities of the robot and scattered objects.

Initialization. The robot is initialized to a standing position. The scattered objects’ positions are randomly initialized within a specific area. Random noise is added to all joint positions during each episode reset.

Reward Implementation. Let

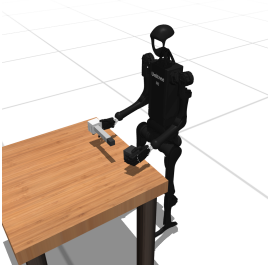
- X be a matrix containing the location of all scattered objects in 3D coordinates.
- $cleanness = tol(\max(Var(X_{:,0}), Var(X_{:,1})), (0, 0), 3)$, where $Var(X_{:,0})$ is the variance of x -coordinates of all objects’ locations, and $Var(X_{:,1})$ is such variance for y -coordinates.

Then,

$$R(s, a) = 0.2 \cdot stable + 0.8 \cdot cleanness$$

Termination. The episode terminates after 1000 steps, or when $z_{pelvis} < 0.3$.

27) *insert*:



Objective. Insert the ends of a rectangular block into two small pegs. Two versions, *insert_small* and *insert_normal* present different object sizes.

Observation. Joint positions and velocities of the robot, rectangular block to insert, and two provided small pegs.

Initialization. The robot is initialized to a standing position. The rectangular block and two pegs are initialized on the table at specific orientation and position.

Reward Implementation. Let the rectangular blocks be formulated to have two ends end_a, end_b , which must be respectively inserted to the pegs peg_a, peg_b .

- $proximity_{peg,site} = tol(d(peg, site), (0, 0), 0.5)$
- $proximity_{block} =$

$$mean(proximity(peg_a, end_a), proximity(peg_b, end_b))$$

- $height(peg) = tol(z_{peg} - 1.1, (0, 0), 0.15)$
- $height_{pegs} = mean(height(peg_a), height(peg_b))$
- $proximity_{hands} =$

$$mean(proximity(peg_a, hand_{left}), proximity(peg_b, hand_{right}))$$

The reward of this task is phrased as:

$$R(s, a) = (0.5 \cdot stable + 0.5 \cdot proximity_{block}) \times (0.5 \cdot height_{pegs} + 0.5 \cdot proximity_{hands})$$

Termination. The episode terminates after 1000 steps, or when any of the blocks or pegs are at a height lower than 0.5 from floor.

APPENDIX C TRAINING DETAILS

A. Baseline Implementation Details

For SAC, we use the implementation from JaxRL Minimal [13]. For PPO, we use the Stable-Baselines3 [44] implementation with 4 parallel environments. For DreamerV3 and TD-MPC2, we use their official code. For DreamerV3, we use the ‘medium’ configuration, with an update-to-data ratio of 64. For TD-MPC2, we use the 5M configuration. Unless specified, we use their default hyperparameters.

B. Reaching Policy Implementation Details

We train the low-level reaching policies described in Section V-D using PPO, largely parallelized on GPU using MuJoCo MJX. We employ the PureJaxRL [30] implementation, using their default parameters, except a higher number of environments as detailed in Section V-D, 16 steps per environment, and an entropy coefficient of 0.001.

C. Benchmarking Results

We summarize our benchmarking results in Table III and Table IV . We report the mean and standard deviation of maximum episode returns over three seeds. DreamerV3 and SAC are trained for 10M while TD-MPC2 is trained for 2M environment steps, which roughly corresponds to 48 h.

	DreamerV3	TD-MPC2	SAC	Target
walk	800.2 ± 158.7	782.0 ± 109.2	31.7 ± 24.0	700.0
stand	622.7 ± 404.8	809.0 ± 137.1	208.3 ± 105.6	800.0
run	633.8 ± 222.4	93.3 ± 14.3	5.0 ± 2.1	700.0
reach	7580.9 ± 1951.0	7316.1 ± 2112.1	4565.1 ± 212.8	12000.0
hurdle	126.2 ± 59.4	46.4 ± 10.8	13.2 ± 8.8	700.0
crawl	878.8 ± 122.7	957.4 ± 17.5	330.0 ± 111.9	700.0
maze	272.3 ± 116.6	244.3 ± 97.7	144.8 ± 17.8	1200.0
sit_simple	891.4 ± 38.4	411.1 ± 368.0	148.3 ± 103.8	750.0
sit_hard	433.4 ± 355.9	343.0 ± 381.7	55.0 ± 18.2	750.0
balance_simple	19.8 ± 7.0	40.5 ± 23.9	61.5 ± 1.1	800.0
balance_hard	45.9 ± 27.4	48.2 ± 28.5	42.5 ± 22.6	800.0
stair	131.1 ± 43.6	70.4 ± 7.1	14.1 ± 6.8	700.0
slide	436.5 ± 200.1	119.0 ± 35.9	6.3 ± 2.8	700.0
pole	658.3 ± 343.3	226.3 ± 116.1	46.3 ± 26.4	700.0
push	-1251.9 ± 659.8	-258.7 ± 66.5	-97.9 ± 147.0	700.0
cabinet	57.3 ± 66.3	112.8 ± 142.9	211.8 ± 33.8	2500.0
highbar	8.9 ± 5.8	0.3 ± 0.0	9.4 ± 3.7	750.0
door	213.0 ± 149.3	274.7 ± 12.5	39.4 ± 25.2	600.0
truck	1103.8 ± 232.9	1132.6 ± 72.1	1077.5 ± 95.0	3000.0
cube	111.2 ± 59.9	54.7 ± 33.1	130.7 ± 30.5	370.0
bookshelf_simple	840.4 ± 5.6	136.2 ± 71.6	346.9 ± 231.5	2000.0
bookshelf_hard	530.2 ± 302.5	37.0 ± 1.3	293.9 ± 121.6	2000.0
basketball	19.3 ± 2.5	42.0 ± 14.8	22.1 ± 3.2	1200.0
window	461.0 ± 252.8	87.1 ± 37.5	62.9 ± 83.8	650.0
spoon	349.7 ± 46.2	77.9 ± 80.6	87.7 ± 80.5	650.0
kitchen	0.0 ± 0.0	0.0 ± 0.0	0.0 ± 0.0	4.0
package	-18015.2 ± 9477.7	-3655.6 ± 1055.0	-6718.3 ± 607.0	1500.0
powerlift	315.9 ± 16.9	99.1 ± 47.3	81.8 ± 46.7	800.0
room	120.5 ± 71.4	131.4 ± 56.7	12.0 ± 4.9	400.0
insert_small	184.8 ± 26.3	129.8 ± 51.9	10.8 ± 13.4	350.0
insert_normal	171.5 ± 33.2	237.6 ± 9.1	46.3 ± 63.1	350.0

TABLE III: Average returns for HumanoidBench. Each number represents average return@10M (return@2M) with the standard deviation for DreamerV3 and SAC (TD-MPC2).

	DreamerV3	TD-MPC2	SAC	Target
walk	932.4 ± 0.3	900.3 ± 47.6	68.7 ± 27.0	700.0
stand	932.9 ± 1.1	925.7 ± 2.5	809.9 ± 194.5	800.0
run	895.9 ± 6.0	226.7 ± 23.3	104.8 ± 7.4	700.0
reach	9831.6 ± 115.9	9727.6 ± 48.9	7169.9 ± 874.1	12000.0
hurdle	396.8 ± 39.7	196.7 ± 30.5	78.6 ± 32.8	700.0
crawl	985.3 ± 0.6	985.2 ± 0.4	626.5 ± 29.1	700.0
maze	592.5 ± 49.0	444.9 ± 22.1	269.9 ± 37.8	1200.0
sit_simple	935.7 ± 5.5	928.4 ± 1.5	842.7 ± 50.8	750.0
sit_hard	914.6 ± 1.5	906.3 ± 6.0	214.0 ± 47.9	750.0
balance_simple	95.4 ± 8.3	95.3 ± 3.1	80.7 ± 3.7	800.0
balance_hard	114.0 ± 12.3	122.2 ± 13.1	71.0 ± 7.9	800.0
stair	411.4 ± 9.7	251.9 ± 9.1	42.8 ± 0.7	700.0
slide	928.4 ± 2.0	311.9 ± 15.1	41.4 ± 2.4	700.0
pole	952.2 ± 10.3	644.9 ± 21.2	440.0 ± 88.4	700.0
push	1000.0 ± 0.0	1000.0 ± 0.0	352.8 ± 31.5	700.0
cabinet	722.6 ± 7.3	721.6 ± 25.9	485.9 ± 137.2	2500.0
highbar	83.1 ± 4.6	0.9 ± 0.4	40.8 ± 41.7	750.0
door	335.7 ± 14.8	310.6 ± 10.6	251.2 ± 9.0	600.0
truck	1674.3 ± 52.6	1457.2 ± 24.3	1387.5 ± 10.0	3000.0
cube	237.9 ± 3.4	241.1 ± 1.2	203.5 ± 27.2	370.0
bookshelf_simple	849.6 ± 0.3	825.0 ± 9.6	766.5 ± 10.3	2000.0
bookshelf_hard	867.8 ± 8.4	320.4 ± 58.9	681.5 ± 10.3	2000.0
basketball	808.8 ± 340.5	1055.3 ± 4.1	192.3 ± 45.6	1200.0
window	765.6 ± 38.4	201.1 ± 91.5	128.6 ± 170.8	650.0
spoon	421.5 ± 2.5	403.5 ± 3.2	297.5 ± 26.5	650.0
kitchen	0.0 ± 0.0	0.0 ± 0.0	0.0 ± 0.0	4.0
package	1009.2 ± 4.1	1003.3 ± 3.4	-3552.8 ± 361.3	1500.0
powerlift	338.6 ± 0.1	264.7 ± 23.9	171.2 ± 3.6	800.0
room	420.8 ± 51.1	353.3 ± 41.5	52.2 ± 3.9	400.0
insert_small	239.8 ± 4.6	226.4 ± 10.8	72.7 ± 21.9	350.0
insert_normal	279.9 ± 9.9	273.0 ± 5.7	135.3 ± 51.5	350.0

TABLE IV: Maximum returns for HumanoidBench. Each number represents maximum return@10M (return@2M) with the standard deviation for DreamerV3 and SAC (TD-MPC2).